Effects of afforestation and crop systems on the water balance in the highlands of Ethiopia

Rebecca Naomi ter Borg

Master´s thesis • 30 ECTS
Swedish University of Agricultural Sciences, SLU
Faculty of Natural Resources and Agricultural Sciences / Department of Soil and Environment
Soil, Water and Environment – Master's Programme
Examensarbeten, Institutionen för mark och miljö, SLU, 2020:09
Uppsala 2020

Effects of afforestation and crop systems on the water balance in the highlands of Ethiopia

Rebecca Naomi ter Borg

Supervisor: Jennie Barron, SLU, Department of Soil and Environment
Examiner: Sigrun Dahlin, SLU, Department of Soil and Environment

Credits: 30 ECTS
Level: Second cycle, A2E
Course title: Master thesis in Soil Science, A2E
Course code: EX0880
Programme/education: Soil, Water and Environment - Master's programme
Course coordinating dept: Department of Soil and Environment

Place of publication: Uppsala
Year of publication: 2020
Title of series: Examensarbeten, Institutionen för mark och miljö, SLU
Part number: 2020:09

Keywords: *Acacia decurrens,* landscape water balance, sediment yield, soil and water conservation, SWAT modelling, water balance partitioning

Swedish University of Agricultural Sciences
Faculty of Natural Resources and Agricultural Sciences
Department of Soil and Environment

Archiving and publishing

Approved students' theses at SLU are published electronically. As a student, you have the copyright to your own work and need to approve the electronic publishing. When you have approved, metadata and full text of your thesis will be visible and searchable online. When the document is uploaded it is archived as a digital file.

[X] YES, I hereby give permission to publish the present thesis in accordance with the SLU agreement regarding the transfer of the right to publish a work. https://www.slu.se/en/subweb/library/publish-and-analyse/register-and-publish/agreement-for-publishing/

[ ] NO, I do not give permission to publish the present work. The work will still be archived and its metadata and abstract will be visible and searchable.

Abstract

In the Upper Blue Nile Basin land use is rapidly changing due to agricultural development and intensification with potential effects on the water availability both up- and downstream. This study is aimed to explore the impact of agricultural land use change on a landscape water balance. The studied watershed in the Fagita Lekoma District, Ethiopia has undergone agricultural change from an annual cropping system to an afforestation system with *Acacia decurrens* plantations. The land use has significantly changed from dominant crop and pasture on almost 90% of the area to permanent cultivated or natural forest on >45% of the area over the last 20 years.

The soil water assessment tool (SWAT), a distributed dynamic model was set up to analyse the effects of land use change on the water balance and sediment yields. Three scenarios were run; a control, a control with improved soil water conservation (SWC) practices and the land use with the afforestation practices.

The modelling resulted in some unexpected changes on the actual evapotranspiration (ET_a) and surface runoff between the control and afforestation practices. Due to a high biomass density of the plantations a higher ET_a and a lower surface runoff were expected. But the *A. decurrens* dominated landscape showed less ET_a than the control dominated by annual crops. The water balance is sensitive to the designed growth response parameters of the *A. decurrens*. Between the control and the control with improved SWC practices there was no significant change in the landscape water balance. The implementation of the afforestation practice and SWC practices reduced the sediment yields in the watershed from 26.5 to 15.5 t ha^{-1} y^{-1}. Cropland was the land use that in all scenarios was most prone to soil erosion.

It is likely that the *A. decurrens* crop description has affected the modelled water balance. Therefore, next steps should be field verification of growth response parameters and water and nutrient uptake parameters. Furthermore, higher resolution input data needs to be acquired to support calibration and validation of the model.

Keywords: Acacia decurrens, afforestation, landscape water balance, sediment yield, soil and water conservation, SWAT modelling, water balance partitioning

Popular science summary

Along the river Nile, many people are dependent on its water for household, agriculture and industrial purposes. Variations in rainfall upstream might cause droughts or floods in dry downstream areas. One of the most important sources of water in the Nile River are the Ethiopian Highlands. About 85% of the Nile water originates in the highlands. Ethiopia is highly dependent on rainfed agriculture which is characterized by low crop production. Sustainable development is needed to guarantee higher crop yields and enough water for downstream areas.

In the Ethiopian Highlands land degradation is another big issue. Through soil erosion a lot of sediment is lost each year. Besides soil erosion, the depletion of nutrients in the soil has led to a decrease in soil fertility. The decreasing soil fertility in return has led to a lower agricultural productivity.

In the Ethiopian Highlands, forest has made way for agriculture because of an increasing population pressure on food, energy and resources. One of the consequences of deforestation is the increase in land degradation. The trend is in some areas reversing, like in the Fagita Lekoma District in the northwestern highlands. 20 years ago agriculture in the district was dominated by crop production. Nowadays annual crops are still dominating but *Acacia decurrens* trees are planted to prevent further land degradation and improve livelihoods by generating extra income through charcoal production. This afforestation practice has unknown consequences on the water balance and soil erosion.

The change from a cropping system to an afforestation system was modelled for a watershed in the Fagita Lekoma District with a soil water crop model. Climate, elevation, soil, vegetation and land use data were used to model the watershed. This study showed no major differences in the water balance because of the changed practice. But the evapotranspiration was lower than expected, this was probably caused by the tree description of the *Acacia decurrens* in the model. Because of the high leaf biomass of the trees a higher evapotranspiration was expected. There are also signs that through the year the flow to the stream is steadier in the watershed with the afforestation practice, what will be good for areas further downstream. The soil erosion has been reduced in the watershed with the afforestation practices. Areas with crops still experience high rates of soil erosion. The description of the *Acacia decurrens* has most likely impacted the water balance in this study. Research and field measurements will need to be done to improve the model in the future.

Table of contents

List of tables

List of figures

Abbreviations

A. decurrens	*Acacia decurrens*
AfSIS	African soil information service
AWC	Available water capacity
BLAI	Maximum potential leaf area index
CEC	Cation exchange capacity
DBH	Diameter at breast height
DEM	Digital elevation model
ET_a	Actual evapotranspiration
ET_p	Potential evapotranspiration
FAO	Food and Agriculture Organization of the United Nations
GERD	Great Ethiopian Renaissance Dam
HRU	Hydrological response unit
K factor	Erodibility factor
K_{sat}	Saturated hydraulic conductivity
LAI	Leaf area index
MERRA	Modern-era retrospective analysis for research and applications
MUSLE	Modified universal soil loss equation
N	Nitrogen
P	Phosphorus
RUE	Radiation-use efficiency
SPI	Standard precipitation index
SSA	Sub-Saharan Africa
STD	Standard deviation
SWAT	Soil and water assessment tool
USLE	Universal soil loss equation
WRB	World reference base

1. Introduction

The water of the Nile River is an essential resource for the livelihood of 257 million people (NBI 2016). The Upper Blue Nile Basin in the highlands of Ethiopia is one of the main tributaries to the Nile River. Of the water flow of the Nile River 85 % originates in the Ethiopian Highlands, of which 60% comes from the Blue Nile River (Abbay River). The Blue Nile River is together with the Tekeze River the main source of sediments to the Nile River (NBI 2016). These water and sediment flows are highly seasonal. On average 48.9 Gm^3 y^{-1} of water is discharged by the Upper Blue Nile to the Nile River (Dile *et al.* 2018). The Ethiopian Highlands and the equatorial region of the Nile Basin receives the most rainfall while other areas are experiencing hyper-arid and sub-humid conditions (Onyutha 2016). Changes in water quantity and water quality in the Upper Blue Nile Basin can have major ramifications further downstream on water supply, food security and land use management (Mellander *et al.* 2013; Elsanabary & Gan 2015; Jung *et al.* 2017).

The Upper Blue Nile Basin has also a great potential when it comes to hydropower and agricultural intensification, but the high water dependency of downstream regions leads to conflict (Allam *et al.* 2016). At the moment the Great Ethiopian Renaissance Dam (GERD) is being constructed close to the border between Sudan and Ethiopia. The filling of the 1883 km^2 (73 Gm^3) GERD reservoir will take several years, during which a part of the annual flow will be reduced. There is no publicly declared policy for the filling of the reservoir but it will impact the streamflow to downstream countries for at least five to fifteen years dependent on the annual release of water (Abtew & Dessu 2019a). Besides the construction of the GERD, the utilization of water is growing in the Upper Blue Nile Basin. The impact of environmental degradation and changes in land use and management can most likely also cause a reduced flow to the Nile River (Abtew & Dessu 2019b).

The land use in the Upper Blue Nile Basin is rapidly changing due to agricultural development and intensification. Only a few studies are looking at the effects of land use change and water resource impacts on landscape scale. Studies have been conducted on the hydrology of the Upper Blue Nile Basin. Many studies focus on the Upper Blue Nile Basin (Gebrehiwot *et al.* 2011; Tekleab *et al.* 2011), the Lake Tana Basin (Kebede *et al.* 2006; Setegn *et al.* 2008; Lemma *et al.* 2019) or sub-catchments of the Upper Blue Nile Basin (Asmamaw & Mohammed 2013; Dile *et al.* 2013a; Worqlul *et al.* 2018). Most of the hydrological studies in the Upper Blue

Nile Basin are conducted on the Lake Tana Basin (Senkondo *et al.* 2018; Worqlul *et al.* 2018). Senkondo *et al.* (2018) categorized the distribution of studies in East Africa per drainage basin size. Most studies have been performed on a spatial scale of 1,000 – 10,000 km^2. At a sub-catchment scale, the understanding of hydrological processes is often lacking (Tekleab *et al.* 2011). It is important to consider spatio-temporal variations in hydrological processes when developing a model and a certain level of uncertainty in model predictions should be expected due to insufficient knowledge of basin behaviour (Senkondo *et al.* 2018). Spatial and temporal variability of climate, topography, soil and geology in Ethiopia have a significant impact on the water availability (Berhanu *et al.* 2014). Many studies conducted in the Upper Blue Nile Basin mention a lack of information on hydrological and soil properties. Smaller catchments are often ungauged and weather stations are irregularly positioned.

Agricultural activities are important for Ethiopia's economy where land use changes and climate change can cause serious challenges for the environment (Dereje Ayalew 2012; Berihun *et al.* 2019). Agricultural practices in the Upper Blue Nile Basin are mainly rainfed and have low input – output features (Dile *et al.* 2016). The high population density in the Ethiopian Highlands puts a lot of pressure on the natural resources and land is converted rapidly from forests to agricultural land (Belayneh *et al.* 2018).

Given the importance of weighting upstream and downstream water resources and water use in the Nile Basin, this study looks at a case of rapidly changing agriculture land use and the possible impacts on a landscape water balance.

1.1. Aim of the study

The aim of this study is to explore the impact of agricultural land use change on a landscape water balance. This study is conducted on a watershed in the Fagita Lekoma District, Ethiopia. The land use in the Fagita Lekoma District has changed over the last couple of decades from annual cropping to an afforestation system through a farmer driven process. To date some studies of farmer benefits and implications on land cover change have been executed (Nigussie *et al.* 2017a; b, 2020; Belayneh *et al.* 2018; Wondie & Mekuria 2018). However, there is no estimates on the impacts on water balance partitioning and water use, nor sediment loads, which are important environmental factors that impact the upstream and downstream areas. The following key research questions were explored during this study with the distributed dynamic model called the soil water assessment tool (SWAT), for a thirty year period:

1. How has the land use in the watershed in the Fagita Lekoma District changed in the last twenty years?

2. How does water balance partitioning change under different types of meso scale vegetation from annual crops to rotational afforestation practice?
3. Do field scale soil and water conservation practices affect the landscape water balance partitioning in a slope catchment?
4. What is the impact of land-use change from annual cropping to afforestation on sediment yields?

2. Background

2.1. Agricultural land use change in Ethiopia

The economy of Ethiopia is mainly based on agriculture. About 85% of the population is employed in the agricultural sector (FAO 2020). Most of the agriculture in Ethiopia is rainfed (FAO 2016) and as a consequence subjected to natural high rainfall variability (Rockström *et al.* 2003). The rainfed agriculture in the Nile Basin is often characterized by low crop yields (NBI 2016). Sustainable intensification of agriculture is a challenge that Ethiopia faces today and improvements of productivity are needed (Dile *et al.* 2013b). The second challenge Ethiopia is facing is the extreme land degradation due to soil erosion and depletion of soil nutrients (Abera *et al.* 2020).

Between 1990 and 2015 Ethiopia has lost approximately 17% of its forest cover, which is equivalent to more than 2.6 million ha (Belayneh *et al.* 2018). Land use conversion, mainly from forest and grazing land into agricultural land, has increased due to a higher demand for food, livestock feed and energy (Tully *et al.* 2015; Belayneh *et al.* 2018; Wondie & Mekuria 2018).

Recently in some parts of Ethiopia, the deforestation trend has been reversed and the implementation of plantations on degraded hillsides has increased (Berihun *et al.* 2019). In the Ethiopian Highlands different kinds of native and exotic species are planted e.g. *Acacia decurrens*, *Chamaecytisus palmensis*, *Eucalyptus globulus*, *Eucalyptus camaldulensis* and *Hagenia abyssinica* (Kindu *et al.* 2006; Tesfaye *et al.* 2015). Eucalyptus is for example cultivated for timber, fuelwood and charcoal but can also severely reduce nutrients in the soil (Liang *et al.* 2016). In the Fagita Lekoma District the *A. decurrens* is planted for short-rotation agroforestry on degraded cultivated land (Nigussie *et al.* 2017a) and exploited mainly for the production of charcoal (Nigussie *et al.* 2020). The *A. decurrens* plantation practices are mainly smallholder plantations (Tadesse *et al.* 2019).

Aerial photography and satellite images are often used to analyse land use change (Zeleke & Hurni 2001). Belayneh *et al*. (2018) have reported annual rates of 18% increase in forest cover in the period 2003 – 2017 in the Fagita Lekoma District, for the same period an annual loss of cropland of 2% was reported. Wondie

& Mekuria (2018) also studied the land use change in the Fagita Lekoma District and found an annual decrease of 1% in forests over 2000 – 2010 and an annual increase of 5% over 2010 – 2015. Furthermore, for the cropland there was an annual decrease of 2% (2000 – 2010) and 1% (2010 – 2015). In both studies there was no differentiation between natural forests and the plantations.

Acacia decurrens

Acacia decurrens, which is introduced in the Fagita Lekoma District, is a nitrogen fixing tree species that finds its origins in Australia. The *A. decurrens* is cultivated in the Wolega and Shoa regions in Ethiopia (Bekele 2007). The *A. decurrens* has been adopted by farmers for improving soil fertility, generating additional income through charcoal production and as a soil and water conservation (SWC) practice (Nigussie *et al.* 2017a). Some other reasons the farmers adopted this practice were that the *A. decurrens* has shallow roots, has little to no effects on the crops and its litter decomposability (Belayneh *et al.* 2018)

The *A. decurrens* is used by farmers in the district in the taungya agroforestry system (Nigussie *et al.* 2017a). In this system the farmers grow crops in the first years together with the trees. The seedlings are spaced at roughly 1x1m and the crops are grown in between e.g. *Eragrostis tef* (teff) *Zea mays* (maize) or *Triticum aestivum* (wheat) (Tadesse *et al.* 2019).

A study on five year old *A. decurrens* plantations in the Fagita Lekoma District showed an increase in soil organic carbon content, organic matter content, total N, available P, CEC and pH and are higher in comparison with cultivated land while the bulk density was lower (Molla & Linger 2017). The same soil quality indicators were studied on *A. decurrens* plantations just before harvesting and also in this case there was an increase in soil quality (Bazie *et al.* 2020).

2.2. Impacts of land use change on the water balance

Studying the water balance of a catchment under land use change is important to understand the potential impacts on water quantity and quality of both surface and groundwater (Tekleab *et al.* 2011). Precipitation, actual evapotranspiration, infiltration, surface runoff and streamflow are important components of the water balance. In the Upper Blue Nile Basin there is a data scarcity when it comes to e.g. observed data. Another problem with the climate data needed for hydrological modelling in the Upper Blue Nile Basin is that meteorological stations are irregularly spaced and have often missing data (Sisay *et al.* 2017).

Impact of land restoration and conservation on runoff, soil loss, soil organic carbon stock and productivity has mainly been studied on plot scale in the Ethiopian Highlands and understanding on landscape scale is limited (Abera *et al.* 2020).

Abera *et al.* mention a runoff reduction of 38-90% across all conditions in a meta-analysis on different land restoration practices.

In a study on hydrological impacts in West-Africa, the long-term simulated runoff due to deforestation increased. As a consequence to the increased runoff, the streamflow increased in this case. Other consequences that generally come with deforestation are soil compaction and decreased infiltration (Li *et al.* 2007). Due to land use change to cropland and grazing land there is an increase in soil bulk density and a decrease in organic matter content visible in many tropical soils and consequently a decrease in infiltration is noticed (Abdelkadir & Yimer 2011). Due to intensive land use the organic matter supply to the soil can be reduced and can affect the soil structure and reduce infiltration (Ilstedt *et al.* 2007).

Advantages of afforestation in Ethiopia are a decrease in soil erosion and sediment yields, and an increase of water infiltration and stream discharge (Lemenih & Kassa 2014). A meta-analysis by Ilstedt *et al.* (2007) showed an increase of infiltration after afforestation and the use of trees in agricultural fields in the tropics. It was also indicated that improvement of soil physical properties is greater in afforestation practices than agro-forestry practices.

2.3. Land degradation in Ethiopia

Globally land degradation is a major problem. Livelihoods in Sub-Saharan Africa (SSA) are particularly threatened since a large part of the population is dependent on agriculture (Tully *et al.* 2015; Nigussie *et al.* 2017a). In fact, Ethiopia is one of the countries that is most affected by land degradation in the world. There are natural and anthropogenic causes that drive land degradation directly or indirectly in Ethiopia; agricultural expansion, wood harvesting, expansion of infrastructure, rainfall variability, population growth, deforestation, soil and water erosion and low technology in agriculture are seen as underlying causes (Birhanu 2014; Megerssa & Bekere 2019).

By soil erosion 1.5 – 2 billion tons of top soil are annually lost and this is one of the main forms of land degradation in Ethiopia (Megerssa & Bekere 2019). The soil losses are estimated to be between 3.4 and 84.5 t ha^{-1} y^{-1} with maximum rates of 300 t ha^{-1} y^{-1} (Abera *et al.* 2020). On cultivated land the soil loss occurs to be higher than for other land uses with a soil loss ranging from 50 t ha^{-1} y^{-1} to 179 t ha^{-1} y^{-1} (Shiferaw & Holden 1999; Adimassu *et al.* 2018; Abera *et al.* 2020). The high levels of soil erosion can also pose a threat to the energy generation by the GERD by reducing the hydropower head (Abtew & Dessu 2019a; Abera *et al.* 2020). Moreover, nationwide nutrient depletion of N, P and K results in lower agricultural productivity (Haileslassie *et al.* 2005).

In Ethiopia several nationwide SWC programs have been undertaken to limit soil erosion. The Food-for-work (1973 – 2002), Managing Environmental

Resources to Enable Transition to more sustainable livelihoods (2003 - 2015), Productive Safety Net Programs (2005 – present), Community Mobilization through free-labour days (1998 – present) and the National Sustainable Land Management Project are some examples of land restoration and conservation initiatives (Haregeweyn *et al.* 2015). The effects of these land restoration efforts are studied. However, due to a lack of comprehensive studies the knowledge of what works where and how is missing (Abera *et al.* 2020).

Tesfaye *et al.* (2018) stated that it is important to identify critical areas to plan and implement soil and water conservation practices. Since many watersheds in the Upper Blue Nile Basin face severe soil erosion it is better to prioritize SWC practices in area that are erosion hotspots.

In a hydrological study using SWAT to model the effects of SWC practices in hotspot areas in Lake Tana Basin, the implementation led to a 59% reduction in sediment yield (Lemma *et al.* 2019). Tesfahunegn *et al.* (2012) simulated in a catchment in the Tigray Region soil erosion for different SWC practices with SWAT. They calculated reductions in soil erosion in comparison with a control of 51% for afforestation. The soils in the Tigray Region are generally however coarser and have higher infiltration rates than the sub humid Upper Blue Nile Basin, where clay soils are more common and there is more precipitation (Tebebu *et al.* 2015).

3. Methodology

In this study the aim was to explore the impacts of land use change on the water balance partitioning and sediment yield. The first part was to find the relevant input data to simulate the water balance and soil erosion in the watershed to examine research question 1:

1. How has the land use in the watershed in the Fagita Lekoma District changed in the last twenty years?

The second part of the study was to build a SWAT model with the input data and created land use maps. With the model three different scenarios were run; a control, a control with improved soil and water conservation practices and land use with the afforestation practices. The controls are according to the 2002 land use and the afforestation practices are under the 2019 land use. The third part was to analyse the model results to respond to the second, third and fourth research question:

2. How does water balance partitioning change under different types of meso scale vegetation from annual crops to rotational afforestation practice?
3. Do field scale soil and water conservation practices affect the landscape water balance partitioning in a slope catchment?
4. What is the impact of land-use change from annual cropping to afforestation on sediment yields?

3.1. Site description

The study area is a small watershed in the north-western highlands of Ethiopia in the Amhara Region (Figure 1). The watershed is located in the Fagita Lekoma and Banja District between latitude 10°58'37,023" and 11°3'28,802"N and longitude 36°50'36,264" and 36°53'23,96"E (WGS_1984_UTM). The watershed area is approximately 31.6 km^2 and the elevation varies between 2,390 and 2,915 meter. The watershed is a part of the South Gojjam subbasin of the Upper Blue Nile Basin which originates in Lake Tana. South Gojjam is one of the fourteen official subbasins in the Upper Blue Nile Basin.

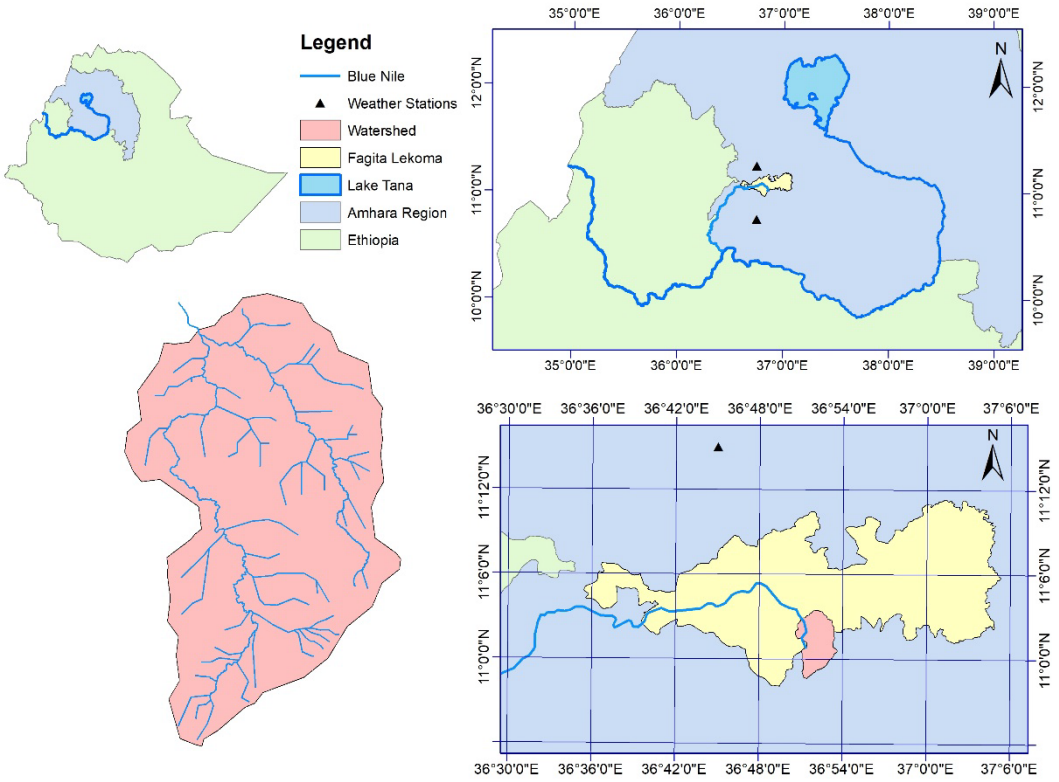

Figure 1. Location of the watershed in the Fagita Lekoma district in Ethiopia. The watershed is part of the Upper Blue Nile Basin.

The Fagita Lekoma District is located in the subtropical agro-ecological zone of the north western highlands. The mean annual rainfall in the district is 2,435 mm (Nigussie *et al.* 2017a) and the mean temperature is around 20°C. There are two rainy seasons in Ethiopia; the *Belg* season and the *Kiremt* season. The *Kiremt* season from June till September contributes most rainfall in the Amhara Region (Gummadi et al. 2018), with the peak rainfall in July and August (Wondie & Mekuria 2018).

Figure 2 shows the mean monthly distribution of precipitation with the standard deviation, potential evapotranspiration and minimum and maximum temperature for 1982 – 2019 (NASA 2018). Based on the datasets used in this study the mean annual rainfall is 1,954 mm y^{-1}. The *Belg* season, from March till May, received approximately 282 mm $season^{-1}$ of rainfall over 1982 - 2019. For the *Kiremt* season, from June till September, this is 1,489 mm $season^{-1}$. The mean potential evapotranspiration (ET_p) is 1,901 mm y^{-1}. The ET_p is calculated based on the climate data by the SWAT model with the FAO Penman-Monteith method (Allen *et al.* 1998). The mean maximum temperature is 26 °C and the mean minimum temperature is 14 °C.

Agriculture is most important activity in the watershed. The major crops in the district are teff, barley, wheat, maize and potato (Belayneh *et al.* 2018; Berihun *et al.* 2019). In the last decade the *Acacia decurrens* has been planted to exploit for

charcoal production. The *A. decurrens* is planted together with a cereal crop at the beginning of the *Kiremt* season. In the second year of the agroforestry rotation, grass is grown with the *A. decurrens* for fodder. After 4 to 5 years, the *A. decurrens* is harvested and charcoal is produced on the fields. Farmers chose to either grow crops for 1 or 2 years or replant the *A. decurrens* the following year.

The dominant soil type in the watershed according to the harmonized world soil database are Humic Nitisols and to a lesser extent Eutric Fluvisols and Haplic Luvisols (FAO *et al.* 2012).

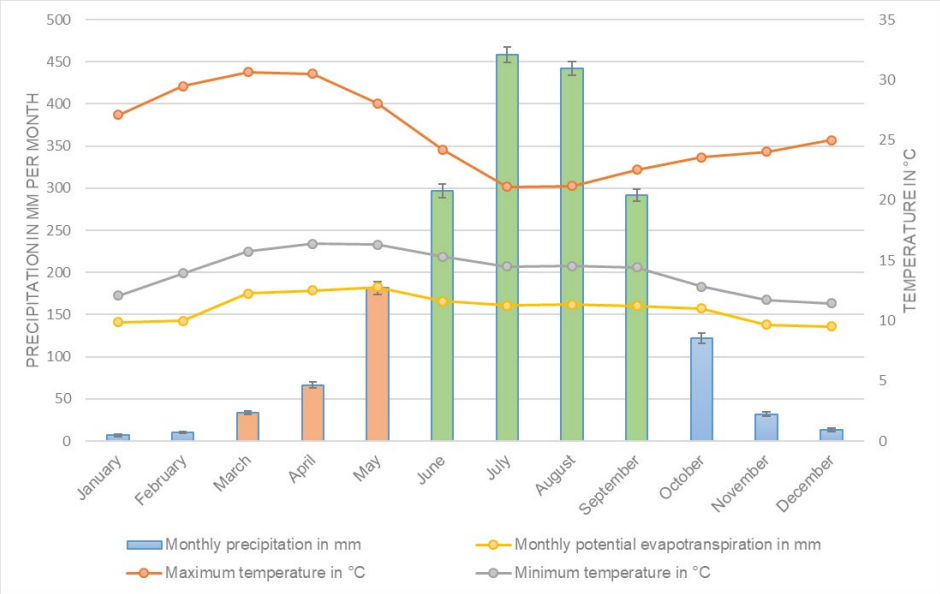

Figure 2. Mean monthly precipitation (Belg season in orange and Kiremt season in green), maximum temperature and minimum temperature over a time period of 1982-2019 at grid point lat. 10.75; long 36.75 (NASA 2018).

3.2. Soil and water assessment tool (SWAT)

To determine the effects of land-use change on the water balance partitioning and sediment loss in the watershed the soil and water assessment tool (SWAT), version SWAT_2012.10_5.21, was used (Arnold *et al.* 2012a). SWAT is a semi mechanistic spatially distributed continuous time soil water crop model. A full model description is available in the theoretical documentation (S.L. Neitsch *et al.* 2011). With SWAT, the long-term impacts of land management practices on hydrology and sediment can be evaluated. Some strengths of the model are the dynamic crop growth and the capacity for a spatially explicit water balance. Because of the dynamic crop growth the water uptake by the vegetation and the actual evapotranspiration are meticulously modelled. In the next subchapters; the methods used to characterize the SWAT input data, the SWAT model set up and the SWAT output data analysis.

Table 1. Required input data for the SWAT model; data description, source, resolution, time and parameters.

	Description	**Sources**	**Resolution, time period**	**Parameters**
DEM	CGIAR-CSI, 2009. SRTM_44_10 Digital Elevation Map. Version 4.1	(Jarvis *et al.* 2008) http://srtm.csi.cgiar.org/	srtm_44_10; 90m x 90m	
Stream network	DEM map processing with ArcMap spatial analysis toolbox (hydrology), Google Earth maps, sampling coordinates, topographic maps accessed through the project *Market-driven afforestation*		90m x 90m	
Climate	MERRA-2 climate data by NASA's Global Modelling and Assimilation Office (GMAO) accessed through the NASA POWER project	(Gelaro *et al.* 2017; NASA 2018) https://power.larc.nasa.gov/data-access-viewer/?fbclid=IwAR0SUp8HH6cpkHlXEWjEDgKkMbeTuKC6VpfOcbfopW7kMUCBnrSzpvwYHpU	Resolution ~50km (Grid) 1982 - 2019	Precipitation, minimum and maximum temperature, wind speed, relative humidity, surface albedo
Soil	Soil maps for the required parameters for 6 soil layers by the Africa soil information service (AfSIS) – ISRIC Data hub. The maps are processed in ArcMap to district and watershed scale.	(Hengl *et al.* 2015) (Leenaars *et al.* 2018) https://www.isric.org/projects/soil-property-maps-africa-250-m-resolution	250m x 250m 1,000m x 1,000m (Grid)	Bulk density, available water capacity, organic carbon, clay, silt, sand and rock content.
Land use/land cover	Processing and analysis of Landsat and Google Earth maps to create land use maps for 2002 and 2019	Landsat imagery accessed through ArcGIS, made available by United States Geological Survey (USGS): https://livingatlas2.arcgis.com/landsatexplorer/ Google Earth imagery	30m x 30 m 10m x 10 m 5m x 5m 2002 and 2019	Natural forest, *Acacia decurrens* plantations, cultivated land, pasture and urban area.
Vegetation	Literature research to determine the crop database parameters for the *Acacia decurrens*.	Multiple literary sources (appendix B) and consultation with experts. (Dye & Jarmain 2004; Kindu *et al.* 2006; Mekonnen *et al.* 2006; Bewket & Teferi 2009; Bulcock & Jewitt 2010; Clulow *et al.* 2011; Arnold *et al.* 2012a; Le Maitre *et al.* 2015; Péllico Netto *et al.* 2015; Tesfaye *et al.* 2015; Gelaro *et al.* 2017; Asmare & Gure 2019; Endalamaw 2019; Ferede *et al.* 2019; Amha *et al.* 2020)		Growth period, radiation-use efficiency, harvest index, leaf area index (LAI), max. canopy height, max. root depth, optimal and minimum temperature for plant growth, Normal fraction of N and P in yield, N and P uptake, min. USLE C factor, max. stomatal conductance, plant residue decomposition coefficient, max. biomass, biomass die-off fraction, root to shoot ratio and light extinction coefficient.

3.2.1. Input data characterisation

For the SWAT model different input data were required to be able to model the water balance partitioning and sediment yield in the watershed. The input data that was required was a digital elevation model (DEM), climate data, land use and vegetation parameters. A summary of this data can be found in table 1.

Digital elevation model and stream network

The DEM for the northwestern part of Ethiopia (SRTM_44_10) was obtained from the CGIAR-CSI website (Jarvis *et al.* 2008). The resolution of the DEM is 90m. In ArcMap 10.4.1 the clip data management tool was used to adjust the DEM to watershed scale.

The next step was to create the stream network for this the hydrology spatial analysis toolbox was used. The flow direction and flow accumulation tools used the DEM to create rasters. A polyline for the streams in the watershed was created from these rasters. The GPS coordinates of the river track of both the Timbile River and the Enkul River were added to ArcMap. With the point to line data management tool polylines were made for both rivers. The polylines of the streams and the rivers were combined to one polyline. The created polyline was compared with the topographic maps of Adis Kidame and Gimja Bet (Ethiopian mapping agency (EMA) 1987a; b) and where needed the polyline was edited. Figure 3 shows the DEM and the created stream network of the watershed.

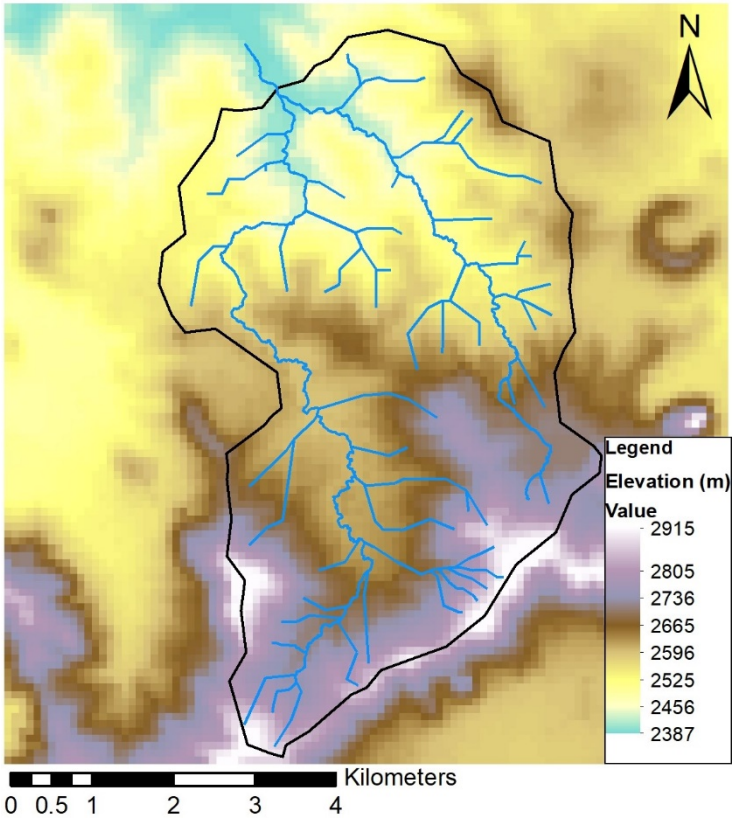

Figure 3. DEM and stream network of the watershed (Jarvis et al. 2008).

Climate

Two climate datasets with daily precipitation, maximum temperature, minimum temperature, relative humidity, solar radiation and wind speed for the time period 1982 to 2019 were downloaded from the NASA POWER project, based on the coordinates of the watershed (NASA 2018). The climate data is MERRA-2 climate data by NASA's Global Modelling and Assimilation Office (GMAO). The two grid points of the MERRA-2 climate data set are located at latitude 10.75 and longitude 36.75 (station 1) and latitude 11.25 and longitude 36.75 (station 2) with an elevation of 1,839 m and 1,864 m. The annual mean precipitation was 1,958 mm y^{-1} for station 1 and 1,949 mm y^{-1} for station 2 with a standard deviation of 397 mm y^{-1} and 412 mm y^{-1}, respectively.

The data for the precipitation, temperature, relative humidity, wind speed and solar radiation were added to separate text files to be able to generate the climate stations in SWAT. The SWAT weather database tool was used to process and run statistics on the weather files and create the monthly weather database (Essenfelder 2018). The weather database was added as WGN_user to the SWAT2012 project database.

Table 2. Soil layers and the corresponding soil physical parameters with the units (Arnold et al. 2012a).

Soil layers	**Properties**	**Units**
0 – 5 cm	Bulk density	g cm^{-3}
5 – 15 cm	Available water capacity	mm H_2O/mm soil
15 – 30 cm	Saturated hydraulic conductivity	mm hr^{-1}
30 – 60 cm	Organic carbon content	% soil weight
60 – 100 cm	Clay content	% soil weight
100 – 200 cm	Silt content	% soil weight
	Sand content	% soil weight
	Rock fragment capacity	% total weight
Top layer	Moist soil albedo	
	USLE soil erodibility (K) factor	(t ha^{-1} h^{-1}) / (ha MJ^{-1} mm^{-1})

Soil

The soil information was obtained in the form of maps from the Africa Soil Profile Database (Africa Soil Information Service (AfSIS) 2015)[1]. The soil maps used describe the physical properties of the soil profile, see table 2 for all the required physical properties (Arnold *et al.* 2012a). The GeoTIFFs have a resolution of 250m. GeoTIFFs are raster images that have metadata and the location embedded. They are in grid format and were downloaded from the ISRIC data hub (Hengl *et al.* 2015; Leenaars *et al.* 2018). The soil maps are available for six soil layers at six intervals. The saturated hydraulic conductivity (K_{sat}) was based on the maps and a hydrology tool and compared with literature (USDA Agricultural Research Service; Hengl *et al.* 2015). A SoilGrids250m GeoTIFF of the world reference base (WRB) subgroup

[1] There are soil maps available of a higher resolution e.g. EthioSIS (Ethiopian Agricultural Transformation Agency). However, these maps were not readily available for the soil physical properties needed in SWAT.

classes was also obtained from the ISRIC data hub (Hengl *et al.* 2017). The soil albedo was obtained from the NASA POWER project (NASA 2018).

Furthermore, the USLE soil erodibility factor or K factor was calculated in ArcMap using equation 3.1. The K factor depends on the soil texture, organic matter content, and soil structure and soil permeability. Equation 3.2 was used to calculate the particle-size parameter (M), where, m_{clay}, m_{silt} and m_{vfs} are the rasters for clay, silt and very fine sand content of the top layer (Hengl *et al.* 2015). The very fine sand content was calculated using the RUSLE2 formula (USDA-Agricultural Research Service 2013; Corral-Pazos-de-Provens *et al.* 2018), equation 3.3, where, m_{sand} is the raster of the sand content of the top layer (Hengl *et al.* 2015). The percentage of organic matter, OM, was calculated with equation 3.4 where org C is the organic carbon content of the top layer (Hengl *et al.* 2015). Based on soil profile descriptions of the Awi Zone, the soil structure or $c_{soilstr}$ is defined as code 4; blocky, platy, prism like or massive (DSA & SCI 2005). Based on literature and the K_{sat}, the soil permeability or c_{perm} is defined as code 5; slow (1-5 mm/hr) (Bayabil *et al.* 2019). The K factor in the watershed varies between 0.087 and 0.156 (t ha^{-1} h^{-1}) / (ha MJ^{-1} mm^{-1}) (figure 4). Similar K factors were found in watersheds in the northwestern highlands of Ethiopia (Bewket & Teferi 2009; Esa *et al.* 2018; Kidane *et al.* 2019).

Figure 4. The USLE soil erodibility factor in the watershed (t ha^{-1} h^{-1}) / (ha MJ^{-1} mm^{-1}) (Hengl et al. 2015).

$$K_{USLE} = \frac{0.00021 \cdot M^{1.14} \cdot (12 - OM) + 3.25 \cdot (c_{soilstr} - 2) + 2.5 \cdot (c_{perm} - 3)}{100} \quad (3.1)$$

$$M = (m_{silt} + m_{vfs}) \cdot (100 - m_c) \quad (3.2)$$

$$m_{vfs} = \left(0.74 - \frac{0.62 m_{sand}}{100}\right) \cdot m_{sand} \quad (3.3)$$

$$OM = 1.72 \cdot orgC \quad (3.4)$$

For the watershed and all the subbasins the average values of the soil physical properties were calculated in ArcMap using the statistical analysis toolbox (Appendix A). For the overall watershed, the user soil ETHIOPIA was created is the project database. The ArcMap values were further processed in MS Excel and added to the soil tables in the SWAT2012 project database to represent the soils per subbasin.

Land use

The land use in the watershed was classified for two different moments in time; before the implementation of *A. decurrens* plantations and after the establishment of *A. decurrens* plantations. Therefore, land use maps were created for 2002 and 2019, for the classification of the land use Google Earth (Google Earth *et al.* 2002; Google Earth & CNES / Airbus 2017, 2019) and Landsat images (ESRI *et al.* 2020) of the growing season for these years were used. With the georeferencing toolbar in ArcMap, the Google Earth and Landsat images were fitted to the display. The image classification toolbar was used to sample the different land uses; agriculture, pasture, natural forest, *A. decurrens* plantations and urban areas. For 2002 the Google Earth map was used as a base for the Landsat images for 2002 were of a poor quality. For 2019 both images were used to create the map. The maps have a resolution of approximately 5m. The land use was analysed on watershed scale. The areas of the different land uses from the SWAT land use report were used to determine the percentage of land cover and calculate the change between 2002 and 2019.

Vegetation

The vegetation that is modelled in the SWAT simulation is based on the land use. The cropland species is defined as *Eragrostis tef* (teff) and are available in the SWAT crop database. However, the root depth of teff was altered from 2 m to 0.75 m (Ayele *et al.* 2001; Tsegay *et al.* 2012). The natural forest and pasture vegetation were also taken from the SWAT crop database.

The *Acacia decurrens* was not in the crop database and parameters needed to be determined. Therefore, literature research was done do to develop the most reasonable crop parameters and where needed experts were consulted. The decision was made to choose parameters for the *Acacia mearnsii* where information was lacking on the *A. decurrens*. The values for the *A. mearnsii* were based on studies in Ethiopia and (sub-) tropical regions around the world. The parameters that could not be determined for the *A. decurrens* nor the *A. mearnsii* were assigned based on other tree crops in the database. In tables 21-24 in appendix B, the complete list with all the crop parameters and sources.

3.2.2. SWAT model setup

The ArcSWAT toolbar in ArcGIS was used to simulate the water balance and erosion in the watershed. In a SWAT project, data is stored in different geodatabases; SWAT project geodatabase, raster storage and SWAT parameter geodatabase. For the different land-use maps different project were created.

Watershed delineator

After the project setup, the first step was the watershed delineation, where the watershed and the subbasins are defined. In the DEM setup, the DEM raster was imported and the stream network was burned in to the DEM, this was done to pre-define the location of the stream network. The stream definition is both DEM-based and based on the flow direction and accumulation; the stream network was added as different layers. The outlet point of the watershed was selected, and based on this the watershed was delineated. The watershed was divided into 27 subbasins.

HRU Analysis

The SWAT hydrologic response units (HRUs) are generated by analyzing the land use, soils and slope (Winchell *et al.* 2013). A HRU is a part of a subbasin that possesses unique attributes when it comes to land use, soil and the slope. A HRU can be scattered in a subbasin but has the same specific land use, soil and slope. (Arnold *et al.* 2012a).

In the land use/soils/slope definition dialog box in the land use data tab, the land use data layer was added in grid format. The data layers for land use in 2002 and 2019 were selected and clipped to the watershed boundary. In the land use classification table, the land cover code were manually defined. Land use was defined as forest-mixed (FRST), *A. decurrens* plantations (ADEC), cropland (TEFF), pasture (PAST) and low density residential areas (URLD). In the soil data tab, the WRB soil data layer was added in grid format and the user soil ETHIOPIA was selected. The user soil ETHIOPIA contains the mean soil physical properties for the watershed as a whole. In the slope tab, the slope was defined in multiple classes, instead of singular, because of the wide slope range. The minimum slope is 0.2%, the maximum slope is 42.0% and the mean is 14.8% with a standard deviation of 7.41%. Based on these statistics, there is chosen to define 5 slope classes of 0-5%, 5-12%, 12-20%, 20-30% and >30%. Based on the DEM the slope classes were calculated by the program. After the land use, soil and slope grids were reclassified an overlay report and an HRU feature class were created. In the report a detailed description on land use, soil and slope distribution is provided for the watershed and the subbasins.

The HRU definition is the final step in the HRU analysis. As a general rule a subbasin should contain 1-10 HRUs, this to simplify the model (Arnold *et al.* 2012a). Multiple HRUs were defined for the watershed, with land use thresholds of 15% (land use over subbasin area), 5% (soil class over land use area) and 15% (slope class over soil area). These thresholds were chosen not to exceed the 10 HRUs. A minimum of 3 HRUs were assigned to the 27 subbasins. In total, there are 135 HRUs assigned for the 2002 land use and 184 HRUs for the 2019 land use. Since the threshold for land use percentage (%) over the subbasin was defined as 15%, any

of the five land uses that has a smaller land cover than 15 % in a subbasin will have no HRU defined for that specific subbasin and will only be defined if the conditions for all three thresholds are met (Her *et al.* 2015). This means that for the URLD no HRUs were defined in the model since the URLD land cover was <1% of the subbasin area.

Write input tables

Firstly, in the weather data definition dialog box, the WGN_user monthly weather database was added to be able to account for any missing climate data. The next step was to add the text files with rainfall, temperature, relative humidity, solar radiation and wind speed data in the respective tabs. After the weather data was defined, the SWAT database tables were written.

Edit SWAT input

Some of the created tables were edited to better represent the land use, HRU or subbasin level of the watershed. Tables that were edited; were the soil tables and management tables. The soil tables were edited because there are differences in soil physical properties according to the soil maps (Hengl *et al.* 2015). In the management tables only the default values were present and needed to represent the HRUs better.

The mean soil values per subbasin, calculated with ArcMap, were added to the soil tables instead of having the soil values for the user soil ETHIOPIA for the whole watershed. However, due to time constraints the land use was not used to optimize the soil data even further and to account for landscape variations.

Table 3. Applied management operations for the different land covers.

Crop	Management operations	Time
Acacia decurrens	Planting beginning of growing season	Year 1; 1 July
	Harvest and kill	Year 6; 1 November
	Planting beginning of growing season (teff)	Year 1; 1 July
	Harvest and kill (teff)	Year 1; 1 December
Eragrostis tef	Planting beginning of growing season	Year 1; 1 July
	Harvest and kill	Year 1; 1 December
	Automated fertilization	Year 1; 1 January
Pasture	Planting beginning of growing season	Year 1
	Grazing	Year 1
	Automated fertilization	Year 1

For the management tables, the management operations for the different land uses were written (table 3) while the forest land use was left unchanged. The automated fertilization function was chosen to limit the nitrogen and phosphorus stress and would only be applied when crops and pasture would be under a certain level of nutrient stress, which was based on several factors. The crops were fertilized with elemental N and P while pastures were fertilized with manure. The nutrient fluxes were for this study not analysed but without the fertilization the model would deplete the soil of nutrients, causing unwanted effects on the pastures and crops. During the modelling it was assumed the *A. decurrens* would be planted every 6 years

without having a year in between agroforestry cycles with an annual crop. There is chosen to let the *A. decurrens* grow for 5 years although farmers also harvest after 4 years. Uprooting of the *A. decurrens* and tillage of the crop fields were due to time and modelling constraints not taken into account, although they do have an impact on the water balance and sediment yields.

Three different land use scenarios were run with the SWAT model. The control is the land use as it was in 2002 before the implementation of plantations in the watershed. No major changes were made for the control, except for the editing of the soil and management tables.

For the afforestation land use, the 2019 land use map was used. In the afforestation scenario the *A. decurrens* trees were added to the crop database. The soil and management tables were like in the control edited. Besides these tables also the SCS runoff curve number or CN value for the *A. decurrens* was lowered from 87 to 79 to match the natural forest CN value. The SCS runoff curve number is dependent on the soil's permeability, land use and soil water conditions.

The third land use scenario is the control scenario with improved soil and water conservation practices. The input data is similar to the control except that terraces were implemented on cropland that has a maximum slope of 20% (Huffman *et al.* 2013). The initial SCS runoff curve number (CN2), the USLE practice factor (USLE_P) and the slope length (SLSUBBSN) were altered to create the terraces (Waidler *et al.* 2009), see table 4. The SWAT manual was used to determine the parameters (Arnold *et al.* 2012a)

Table 4. Changes between the control and the control with improved SWC practices in the management parameters and HRU parameters.

Scenario	CN2	USLE_P	SLSUBBSN (m)
Control	84	1	15 – 61
Terraces	81	0.5 - 1	9 - 31

SWAT simulation

After all tables were written, the SWAT simulation was ran. The simulation was run over 38 years of which 8 years were a warm-up period and no values were calculated during this period. This resulted in 30 years of data on watershed, reach (stream within a subbasin), subbasin and HRU level. The output data was run through SWAT Check to verify whether there were variables that were excessive or perhaps parameter issues. Parameters issues could be excessive sediment loss, long periods of nutrient stress or high water fluxes. The simulation results were added to a SWAT output database for each scenario and for a daily, monthly and yearly time step.

3.2.3. SWAT Output analysis

Water balance partitioning

In SWAT, the water balance equation is used to simulate the hydrological response. Equation 3.6 is the water balance equation, where t is time in days, SW_t is the final soil water content, SW_0 is the initial soil water content, P_i is the precipitation, $Q_{surf,i}$ is the surface runoff,

ET_i is the evapotranspiration, $Q_{perc,i}$ is the percolation and $Q_{gw,i}$ is the return flow or groundwater flow to the stream. All the units are in mm (S.L. Neitsch *et al.* 2011).

$$SW_t = SW_0 + \sum_{i=1}^{t}(P_i - Q_{surf,i} - ET_i - Q_{perc,i} - Q_{gw,i}) \quad (3.5)$$

The SWAT output MS Access databases that were created after the simulations were used to analyse the results. The mean, minimum, maximum, standard deviation and coefficient of variation were calculated and t tests were done to examine the variation and significant difference of the results. For the t tests an α of 0.05 was used. To calculate the water balance partitioning, the mean annual values were taken from the database. In figure 5, a schematic image of the water balance in SWAT. The partitioning of precipitation with actual evapotranspiration, percolation, surface runoff and streamflow were calculated. The same goes for fractions of baseflow and surface runoff that contributed to the streamflow. The streamflow is in SWAT defined as the water yield and consists of the surface runoff, lateral flow and groundwater flow. The groundwater flow is also referred to as the baseflow.

The actual evapotranspiration, surface runoff, streamflow and baseflow were further analysed on a daily and monthly time scale. Parameters were obtained from the access databases and imported in MS Excel and processed. Graphs and tables were produced to visualize the results.

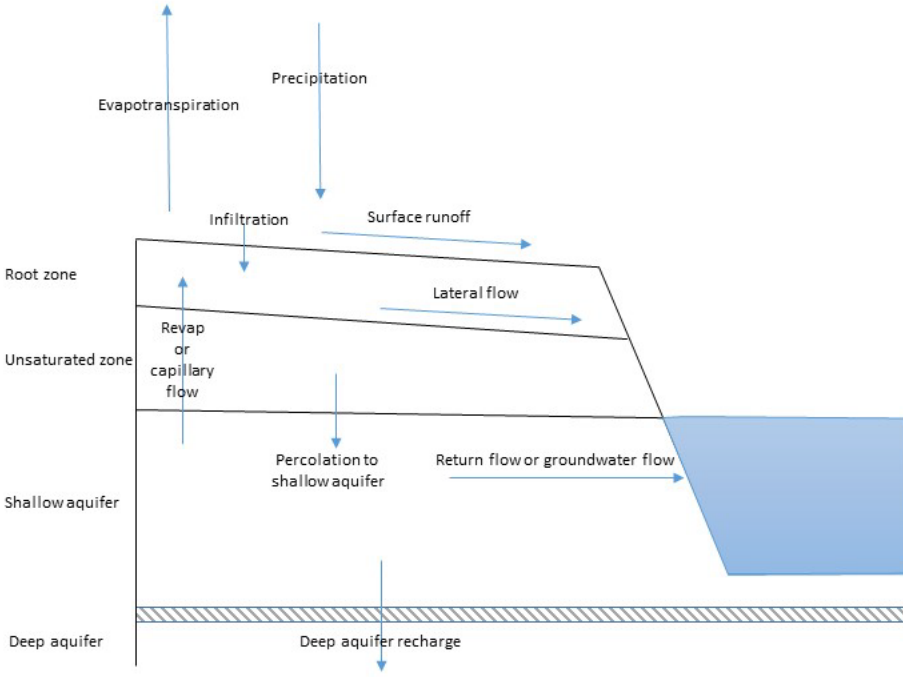

Figure 5. Schematic image of water balance model in SWAT (S.L. Neitsch et al. 2011).

Sediment yield and soil loss

The Modified Universal Soil Loss Equation (MUSLE) is used in SWAT to calculate the soil erosion. Equation 3.7 is the MUSLE for the sediment yield, where SY is the sediment yield, q_p is the runoff peak discharge in m^3/s, A is the HRU area in ha, K is the soil erodibility factor, C

is the land cover/plant factor, LS is the slope length and steepness factor, P is the (soil and water) conservation factor and F is the coarse fragment cover (S.L. Neitsch *et al.* 2011). The energy of the surface runoff is used in the MUSLE rather than the rainfall like in the Universal Soil Loss Equation (USLE) (Vigiak *et al.* 2015). For comparison reasons the SWAT model also calculates the soil loss with the USLE. In the SWAT model, the soil loss is the total amount of soil that erodes from an area, while the sediment yield is the amount of eroded soil that actually ends up in the reach (stream) and will be leaving either subbasin or watershed.

$$SY = 11.8 \cdot (Q_{surf} \cdot q_p \cdot A)^{0.56} \cdot K \cdot C \cdot LS \cdot P \cdot F \quad (3.6)$$

The annual mean sediment yield was calculated in t ha^{-1} y^{-1} on subbasin and HRU level. On subbasin level the change between the control and the SWC scenarios was calculated to determine the reduction. To look closer at the effects of land use change on the sediment yield the mean and standard deviation values were calculated for the different land uses and slopes for all the scenarios. The subbasin and HRU shape files for the scenarios were added to the ArcMap and in the attribute table the calculated sediment yields were added. With use of the symbology tab of the shape file the colouring and range was selected.

3.2.4. Analysis of the rainfall characteristics

The mean and standard deviation (STD) of the annual rainfall for the period 1990-2019 was calculated. The amount of rainfall for the *Belg* and *Kiremt* seasons was determined and the mean and STD were also calculated for the seasons. The maximum precipitation for each year was calculated as well as the number of rainy days. To determine if the climate data from the two stations are significantly different a t-test was run.

For determining the dry and wet periods the standard precipitation index (SPI) was used. Equation 8 was used to calculate the SPI, where, x is the seasonal precipitation, $\bar{x}$ is the long-term mean and σ is the STD of the long-term mean (Mahfouz *et al.* 2016). In table 5, the different drought classes are given. The SPI was calculated for the different years, but was also determined for the *Belg* and *Kiremt* seasons to see which season distributed less rainfall to potential cause a dry season.

$$SPI = \frac{x - \bar{x}}{\sigma} \quad (3.7)$$

Table 5. Drought classes of the standard precipitation index (Asadi Zarch et al. *2015; Elkollaly* et al. *2018).*

SPI range	Drought classes
1.5 – 2	Severely wet
1 – 1.49	Moderately wet
-0.99 – 0.99	Neutral
-1 – -1.49	Moderately dry
-1.5 – 2	Severely dry

4. Results

In section 4.1 the land use change from annual cropping to afforestation that has occurred in the watershed was analysed over the last 17 years. In section 4.2 the rainfall characteristics of the used datasets in the SWAT modelling were analysed. Section 4.3 examined the effects of land use change under different types of meso scale vegetation from annual crops to an afforestation practice. In section 4.4 the impact of land use change on sediment yields in the watershed was examined.

4.1. Change from annual cropping to afforestation in 17 years

During 17 years the watershed has undergone significant land use and land management change, from dominant crop and pasture on almost 90% of the area, to permanent cultivated or natural forest on >45% of the area.

In 2002, the dominant land use in the watershed was an annual cropping system. Although the cropland remains the dominant land use in 2019, there is a clear shift visible (table 6). The land use that is dominating next to the annual crops are the *A. decurrens* plantations.

Table 6. Land cover area and change in land cover area between 2002 and 2019.

Land cover	2002		2019		Change
	Area (ha)	%	Area (ha)	%	%
Pasture	1,034	33	400	13	-61
Eragrostis Teff	1,783	56	1,303	41	-27
Forest	345	11	490	15	42
Acacia decurrens	-	-	967	31	-
Urban/Buildings	-	-	1	0.03	-
Total area	3,162	100	3,161	100	

The areas with annual crops (teff) have decreased by approximately 480 ha. In 2019 approximately 967 ha were covered with *A. decurrens* plantations and were cultivated on land that was previously used for crop production or pastures. However, at some places the *A. decurrens* plantations have replaced areas with natural forest. Furthermore, there is a small increase in natural forest of about 145 ha. On the other hand, there is a decrease of 61% of areas with pastures. In 2002, areas with pastures were dominating in some parts of the watershed. In 2019, the areas with pastures have decreased and cropland and *A. decurrens* plantations seem to have taken over.

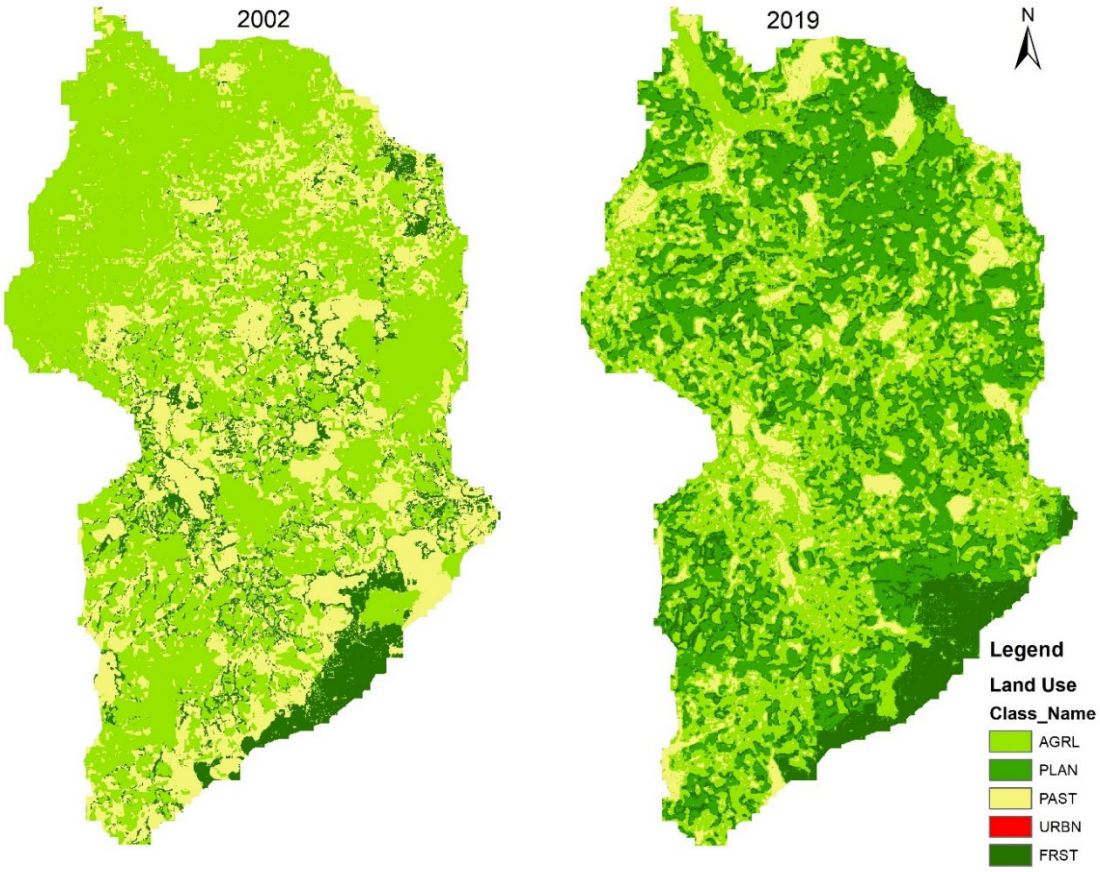

Figure 6. Land use classification for 8 October 2002 and 29 December 2019. Land use is classified as cropland (AGRL), forest (FRST), pastures (PAST), Acacia decurrens plantations (PLAN) and urban (URBN) for the watershed delineated in SWAT.

The land use classification maps for 2002 and 2019 (figure 6) show the spatial distribution of land use in the watershed. The areas with the *A. decurrens* plantations might be underestimated due to the intercropping of seedlings with a cereal crop in the first year of the agroforestry rotation. Only five different land uses were classified in the watershed; cropland, pasture, forest, urban and plantations. However, according to topographic maps (Ethiopian mapping agency (EMA) 1987a) there are some areas with wetlands and ponds in the watershed that were not classified. Some wetlands may be temporary and are only present during the rainy season. According to farmers with the introduction of the *A. decurrens* the wetlands have become drier.

4.2. Rainfall characteristics

There is a high rainfall variability between years and within seasons over the period 1990 – 2019, with a coefficient of variation between 22-23% for the two stations. Half of the daily rainfall is below 5 mm d^{-1}. Only 10% of the rainfall exceeds 20 mm d^{-1}.

The mean annual rainfall is approximately 1900 mm y^{-1} and over the years there is a high variability (table 7). Based on a t-test, the datasets of the two stations are not significantly different. The two tailed t-test showed a p-value of 0.96. The *Belg* season contributes about

14% of the yearly rainfall. However, most rainfall is contributed during the *Kiremt* season, approximately 76% falls during this season. The other 10% of the rainfall is contributed outside of the *Belg* and *Kiremt* seasons.

Table 7. Mean, standard deviation and coefficient of variation (CV) of the annual rainfall, Belg rainfall and Kiremt rainfall.

Weather station	Altitude (m)	Annual rainfall (mm)			*Belg* rainfall (mm)			*Kiremt* rainfall (mm)		
		Mean	STD	CV	Mean	STD	CV	Mean	STD	CV
Station 1	1,839	1,903	434	23	278	122	44	1,443	282	20
Station 2	1,864	1,898	409	22	258	110	43	1,468	280	19

There is no clear trend in the datasets over the period 1990-2019, when looking at the rainfall distribution (figure 7). With the consideration in mind that the mean annual rainfall is approximately 1,900 mm, there are clear dry and wet periods.

Of the 30 years, 18 years have a neutral drought class. The annual and seasonal standard precipitation index (SPI) over the period 1990 – 2019 shows mainly the neutral drought classes with a considerable drought spell in the early 2000s (figure 8). Some of the neutral years have a drier *Belg* season i.e. 1990, 2009 and 2012, whereas others have a wetter *Kiremt* season e.g. 1999 and 2006.

Based on the SPI values, the period 2002 – 2004 is classified as severely dry (figure 8). Furthermore, 2001 and 2011 are classified as moderately dry years. In the period 2001 - 2004 and in 2011 the annual rainfall is lower than the mean *Kiremt* rainfall. With this in mind, there is less than 1150 mm rainfall during the *Kiremt* season for these years. Additionally, for 2002 and 2003 the rainfall during the *Belg* season is also lower than normal.

On the other hand, there are several years that are classified as moderately wet; 1993, 1996, 1997, 2014, 2016 and 2017. The rainfall during the *Kiremt* season is slightly higher for all the moderately wet years except for 1997. For all years, except 1993, there was more rainfall than normal during the *Belg* season.

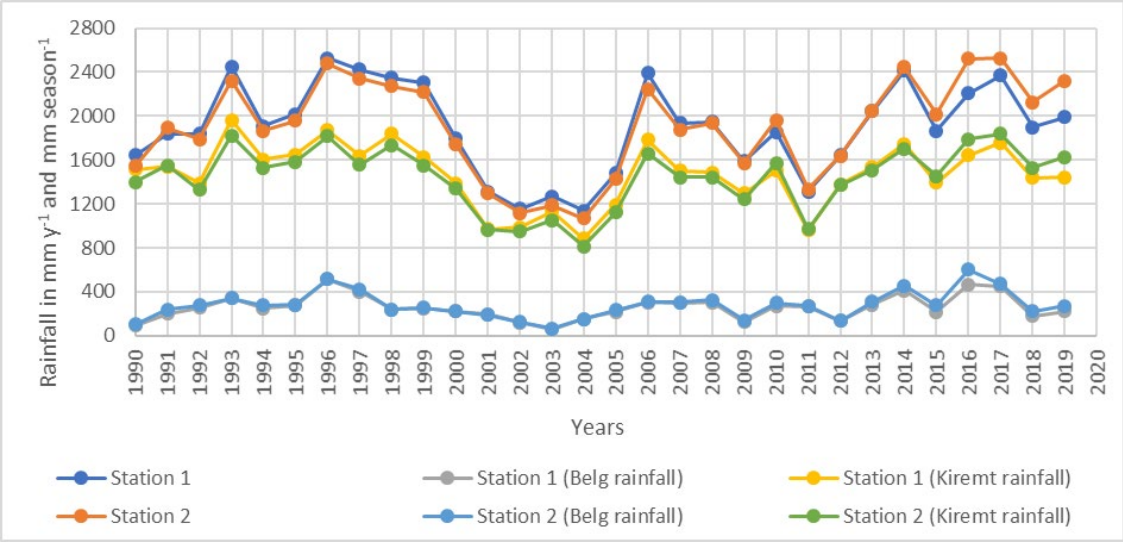

Figure 7. Long-term (1990-2019) annual, Belg and Kiremt rainfall distribution in mm y^{-1} for the 2 weather stations (NASA 2018).

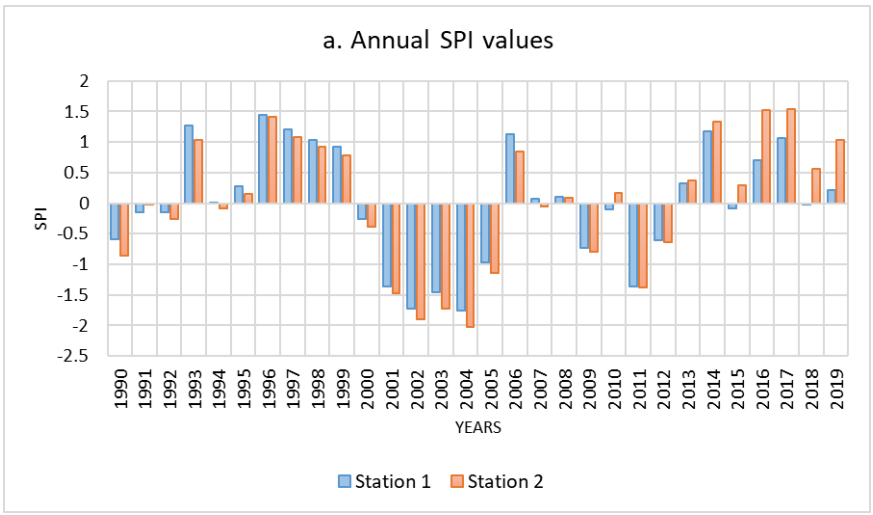

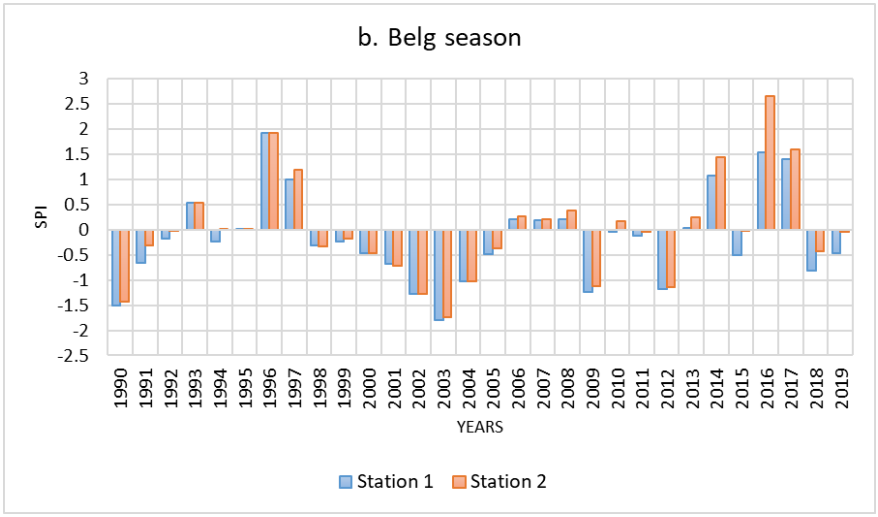

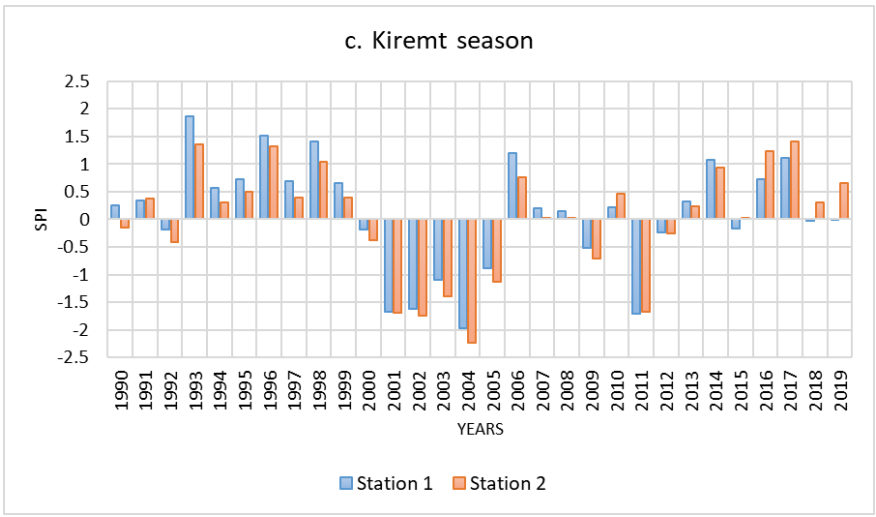

Figure 8. Long-term (1990-2019) annual and seasonal SPI values. The 5 drought classes: 1.5 – 2 severely wet, 1 – 1.5 moderately wet, -1 – 1 neutral, -1 – -1.5 moderately dry and -1.5 – -2 severely dry. SPI values calculated based on data of NASA (2018).

The amount of days with rainfall of more than 0.1 mm d^{-1} lies between 207 and 284 days for station 1 with a mean of 249 days and a STD of 17. For station 2, this lies between 212 and 290 days with a mean of 257 days and a STD of 18. More or less half of the days receive less than 5 mm d^{-1} of rainfall. Approximately 93% of all rainy days receive less than 20 mm d^{-1} of precipitation.

For station 1, the highest maximum daily precipitation was 89 mm d^{-1} in 2015, whereas for station 2 this was 80 mm d^{-1} in 2017. In the period 1990 – 2009, there were only ten days where the rainfall exceeded 50 mm d^{-1}. In the period 2010 – 2019, there were thirteen days that exceeded this threshold. During the period 1990 – 2009, the maximum daily precipitation was 63 mm d^{-1}. However, in the last decade the daily precipitation exceeded the threshold of 80 mm d^{-1} on two consecutive days in 2017 with 88 mm d^{-1} and 82 mm d^{-1}.

4.3. Effects of land use change on the water balance partitioning

The water balance for the landscape under the three different land use and land management practices suggested some unexpected changes in actual evapotranspiration (ET_a) and runoff. The ET_a was for the afforestation scenario 150 mm y^{-1} lower than the control while the runoff was similar for all scenarios. More ET_a and less surface runoff was expected in the afforestation scenario where there was more intensified biomass production. The results of the control and control with improved SWC practices were not significantly different.

Table 8. Long term (1990-2019) annual mean and standard deviation of water balance components for the control, control with improved SWC practices and afforestation land use in mm y^{-1}.

	Control		Soil water conservation		Afforestation	
	Mean	STD	Mean	STD	Mean	STD
Precipitation (mm y^{-1})	1,900	410	1,900	410	1,900	410
Potential evapotranspiration (mm y^{-1})	1,903	40	1,903	40	1,903	40
Actual evapotranspiration (mm y^{-1})	954	91	957	97	803	99
Surface runoff (mm y^{-1})	637	254	589	246	650	257
Lateral flow (mm y^{-1})	18	4	25	4	24	5
Percolation (mm y^{-1})	294	97	328	95	422	119
Groundwater flow (mm y^{-1})	241	90	273	87	362	110
Revap or capillary flow (mm y^{-1})	38	1	38	1	38	1
Recharge deep aquifer (mm y^{-1})	15	5	16	5	21	6
Final soil water content (mm)	211	13	213	13	246	12

The lateral flow, actual evapotranspiration, groundwater flow and percolation in the afforestation scenario were significantly different from the control. On the other hand, there was no significant difference between the control and the control with improved SWC practices. A summary of all the annual means of the different fluxes for all three scenarios can be found

in table 8. In the afforestation scenario the ET_a was approximately 150 mm y^{-1} lower than in the controls. The runoff differed slightly in the three scenarios but were not significantly different. Due to high biomass production and dense canopy of the *A. decurrens* a higher ET_a and less runoff was expected in the afforestation scenario. The percolation and subsequently groundwater flow was significantly higher for the afforestation scenario.

The precipitation ending up as streamflow and baseflow was in the afforestation scenario higher than in the other scenarios, which would be positive for areas further downstream. The higher groundwater flow could have resulted in a higher and steadier baseflow in the stream. For the afforestation scenario about 55% of the precipitation ended up as streamflow. The baseflow in the afforestation scenario was about one third of the total flow in the stream. Consequently, the surface runoff and the lateral flow are contributing the rest of the water to the total flow.

In the next subchapters a comparison between the control and the afforestation scenario for the actual evapotranspiration, surface runoff, streamflow and baseflow. Due to the fact there was no significant difference between the water fluxes of the two controls, there was chosen to not take the control with improved SWC practices into account in this comparison.

4.3.1. Actual evapotranspiration

The actual evapotranspiration (ET_a) was unexpectedly higher in the control in comparison with the afforestation scenario. This was probably a result of the low LAI, dormancy period and sensitive growth response parameters of the *A. decurrens*.

The ET_a for the control was similar for all the years with some slight fluctuations (figure 9). Though, for the afforestation scenario there were differences between the years of the agroforestry rotation. During the first two years of the rotation, the ET_a was similar to the control, while during the remaining four years the ET_a was lower than in the control. From the second year, due to a high leaf biomass of the *A. decurrens,* a higher ET_a was expected for the overall watershed.

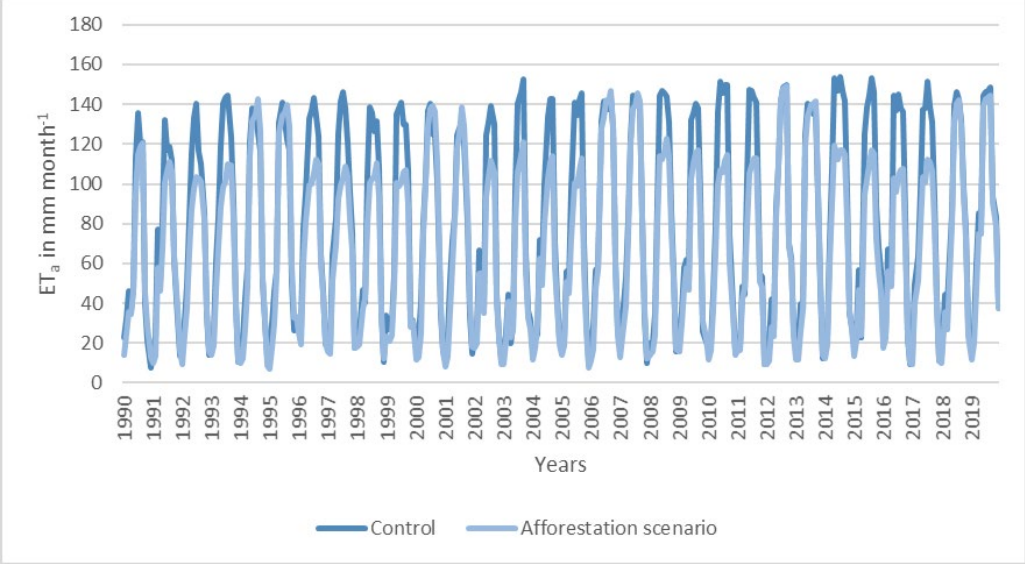

Figure 9. Mean monthly ET_a in mm m^{-1} from 1990-2019 for the control and afforestation land use. The afforestation cycle starts in 1994, 2000, 2006, 2012 and 2018.

In the simulation it was observed that unexpectantly the ET_a for the *A. decurrens* was below the ET_a of the annual cereal crop (figure 10). This was particularly the case during the peak growing season. Furthermore, from the second year of the agroforestry rotation, a LAI of >3 was expected while in the model the LAI did for most years not exceed 2.5. Besides the low LAI, it was also expected that the *A. decurrens* would transpire the entire year, the figures show that at the beginning and end of the year there is an ET_a of practically zero. The low ET_a at the end and beginning of the year can be explained by the tree going into dormancy for just 10 days (day 352 - 361), during which a part of the leaf biomass was lost. Also, the decrease in ET_a around March just before the rainy season might have been caused by water stress.

Moreover, the teff seemed to transpire the entire year. However teff was not planted till day 182 and harvested on day 335 and should only transpire during this period. In figure 10 it looks like the crop is growing for most of the year. There will certainly be evaporation from the soil during the period without a crop, however a similar ET_a as in the beginning of the year was expected.

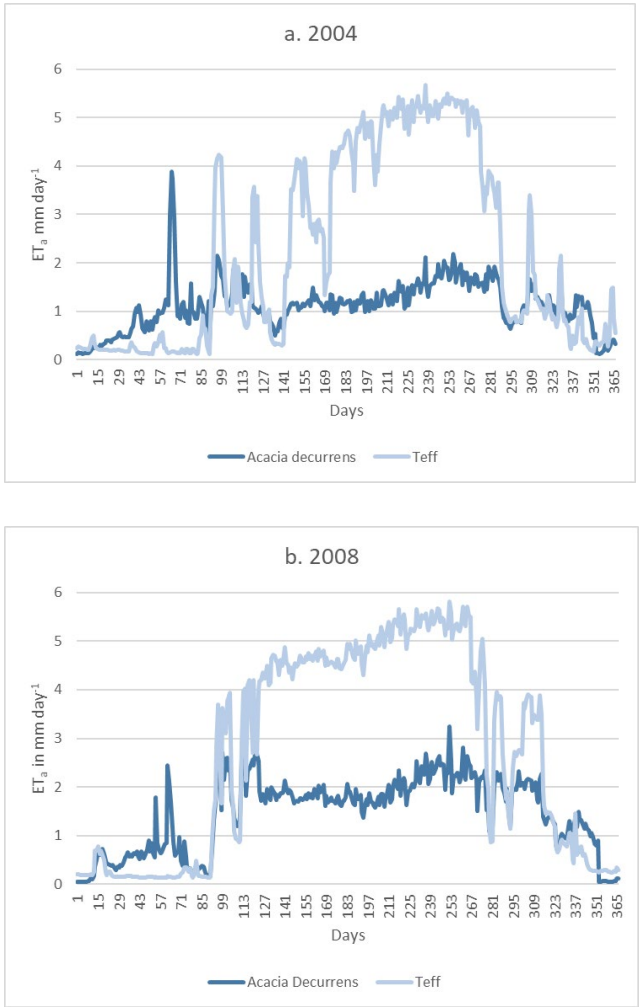

Figure 10. Daily ET_a in mm d^{-1} for the Acacia decurrens and teff in the afforestation scenario for; a. 2004 (dry year), the 3th year of the afforestation cycle and b. 2008 (normal year), the 5th year of the afforestation cycle.

4.3.2. Surface runoff

The surface runoff in the control and the afforestation scenario were similar. Due to the high leaf biomass of the *A. decurrens* it was expected that in the afforestation scenario a larger part of the precipitation would be intercepted by the canopy and less surface runoff would be generated.

In total there were approximately 2,568 surface runoff events over a 30 year period for the control and 2,742 surface runoff events for the afforestation scenario (figure 11). Due to the high LAI, there was the expectation that a part of precipitation would be intercepted for the *A. decurrens* land use and as a result there should be less intense runoff events. However, no such reduction in runoff events could be determined, potentially due to a low LAI for the *A. decurrens* in the model, which was generally not exceeding 2.5.

For the control the runoff events occurred on average 99 d y^{-1}, while for the afforestation scenario this was 104 d y^{-1} (STD: 23 days). Approximately 53% of the events were events with a runoff of 1 – 5 mm d^{-1}. Whereas, 95% of the runoff events were less than 20 mm d^{-1}. On average there were 4 d y^{-1} when the surface runoff exceeded 20 mm d^{-1} for both scenarios. During the dry period between 2001 and 2005 there were in the control only 2 days exceeding 20 mm d^{-1}, while for the afforestation scenario there were 4 days. The six surface runoff events with an intensity of more than 50 mm d^{-1} occurred between 2015 and 2019 except for one event in 1991.

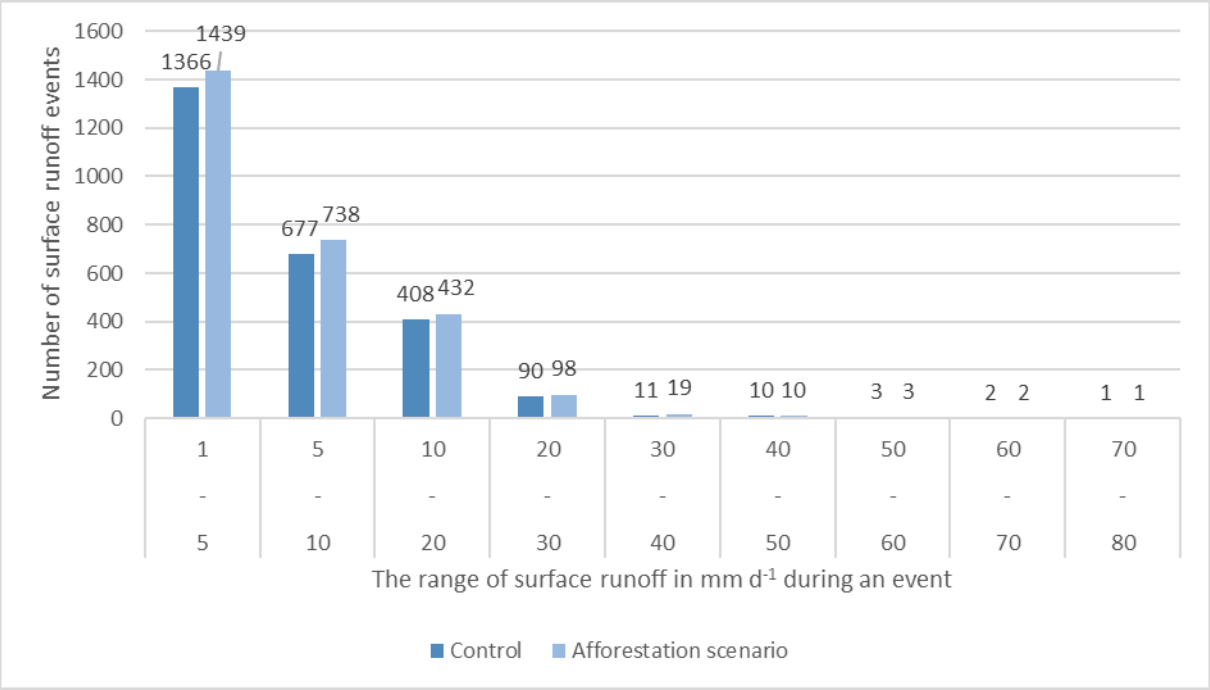

Figure 11. Distribution of surface runoff events with more than 1 mm d^{-1} over 1990-2019 for the control and afforestation scenario.

4.3.3. Streamflow and baseflow

The streamflow was in the control on average lower than in the afforestation scenario. However, the baseflow was significantly different and was steadier and higher through the years for the afforestation scenario.

Table 9. Mean streamflow and baseflow for the control and afforestation scenario in mm y^{-1}.

	Streamflow		Baseflow	
	Mean (mm y^{-1})	STD (mm y^{-1})	Mean (mm y^{-1})	STD (mm y^{-1})
Control	912	39	244	90
Afforestation	1040	85	351	110

As can be seen in table 9, the streamflow and baseflow were higher in the afforestation scenario. The streamflow was lower in the control than in the afforestation scenario. However, the baseflow was significantly different (p-value of 0.0001) from the control and was approximately 44% higher in the afforestation scenario.

The baseflow in the afforestation scenario was higher for most of the year (figure 12). Also the period during the year there was baseflow was longer for the afforestation scenario. The period with baseflow started somewhere during the beginning of the Kiremt season for both scenarios. At the end of the dry season or the beginning of the rainy season there was little to no baseflow for both scenarios depending on the year. In the control there was no baseflow for approximately 129 d y^{-1} while in the afforestation scenario this was 104 d y^{-1} with a coefficient of variation of 23%.

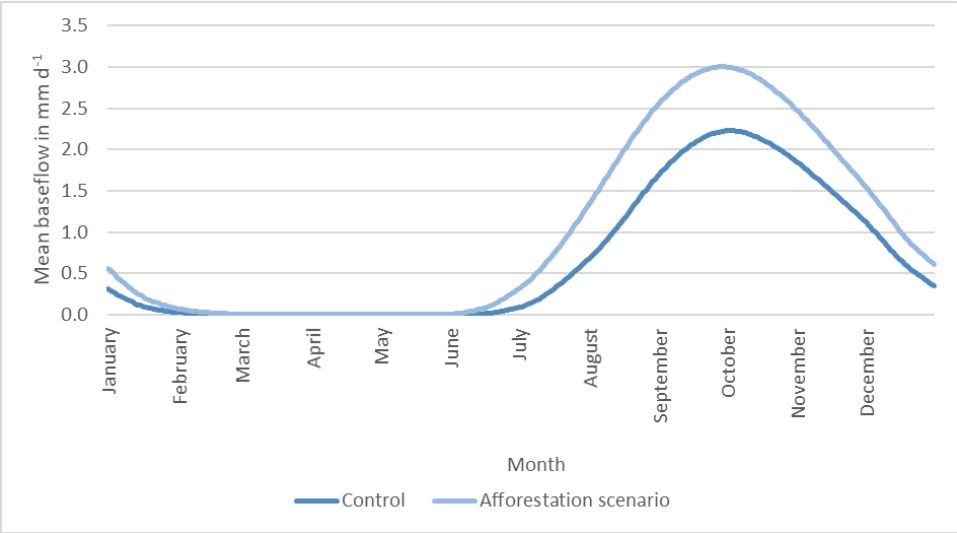

Figure 12. The long-term (1990-2019) mean daily baseflow for the control and afforestation scenario.

4.4. The impact of land use change on the sediment yield

The implementation of soil water conservation practices in the form of the afforestation practice and terraces reduced the sediment yields in the watershed despite the similar runoff. Cropland has the highest sediment yields and was most prone to soil erosion.

The mean annual sediment loadings in the overall watershed were 26.5 t ha^{-1} y^{-1} with a STD of 11.9 t ha^{-1} y^{-1} for the control scenario, 15.3 t ha^{-1} y^{-1} with a STD of 6.9 t ha^{-1} y^{-1} for the control with improved SWC practices and 15.5 t ha^{-1} y^{-1} with a STD of 6.9 t ha^{-1} y^{-1} for the afforestation scenario.

In SWAT, the energy of the runoff was used to determine the sediment yields. As stated before, 95% of the runoff events had an intensity of less than 20 mm d^{-1}. The correlation between the runoff and the sediment yields was plotted in figure 13. As can be seen, the control with improved SWC practices and afforestation scenario show a lower sediment yield with a similar runoff as the control. The maximum sediment yield with a runoff of ≤20 mm d^{-1}, is 2.6 t ha^{-1} d^{-1} for the control, 1.6 t ha^{-1} d^{-1} for the control with improved SWC practices and 1.9 t ha^{-1} d^{-1} for the afforestation scenario. This difference in sediment yields was caused by a difference in the land cover/plant factor (C) and the (soil and water) conservation factor (P) of the MUSLE equation.

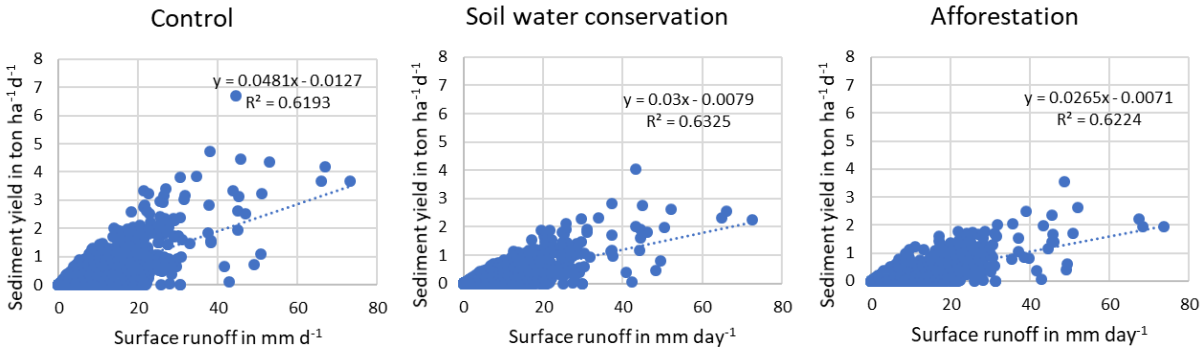

Figure 13. Correlation between surface runoff and sediment yield for the control, control with improved SWC practices and afforestation land use.

To visualize the soil erosion hotspots in the watershed, the sediment yields were determined per subbasin. Between the control and the other scenarios there was a decrease visible in the sediment yield in most subbasins (figure 15).

The highest mean annual sediment yield for the control was 87.4 t ha^{-1} y^{-1} in subbasin 3. For the control with improved SWC practices subbasin 3 also had the highest sediment yield; 59.8 t ha^{-1} y^{-1}. In subbasin 3 cropland was dominating and the slope was > 5%. In the afforestation scenario the highest mean annual sediment yield of 50.5 t ha^{-1} y-1, which was simulated in subbasin 11. Subbasin 11 was dominated by cropland and *A. decurrens* plantations and had a slope of > 5%.

In the control scenario the sediment yields are in general higher than in the two scenarios where SWC practices are applied (table 10). In the control with improved SWC practices there is a reduction in sediment yield of 18 – 62%, with an average reduction of 43%. In the scenario with the afforestation there is a reduction in sediment yields in most subbasins between 3 – 94%. However, in some subbasins in the afforestation scenario the sediment yields have increased i.e. in subbasins 4, 9, 11, 14, 15, 18 and 26. In six subbasins of the afforestation scenario the sediment yield increased with more than 150%. This increase in sediment yield can be explained by the conversion of forest and pasture into cropland and plantations.

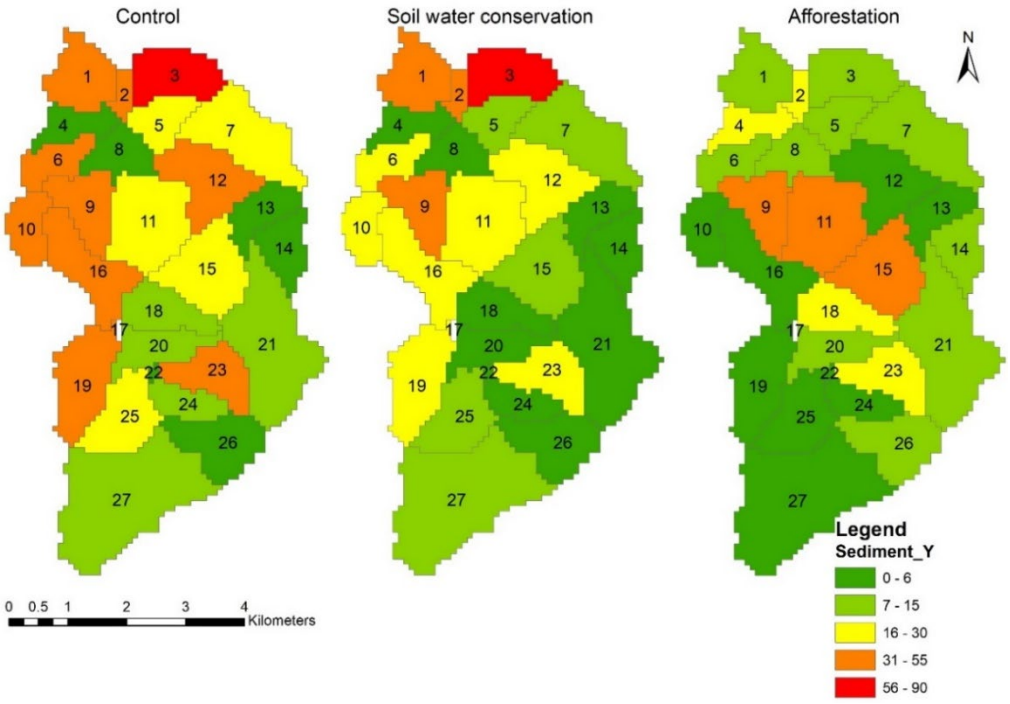

Figure 15. The long-term (1990-2019) average annual sediment yields in t ha^{-1} y^{-1} per subbasin for the control, control with improved SWC practices and afforestation scenario.

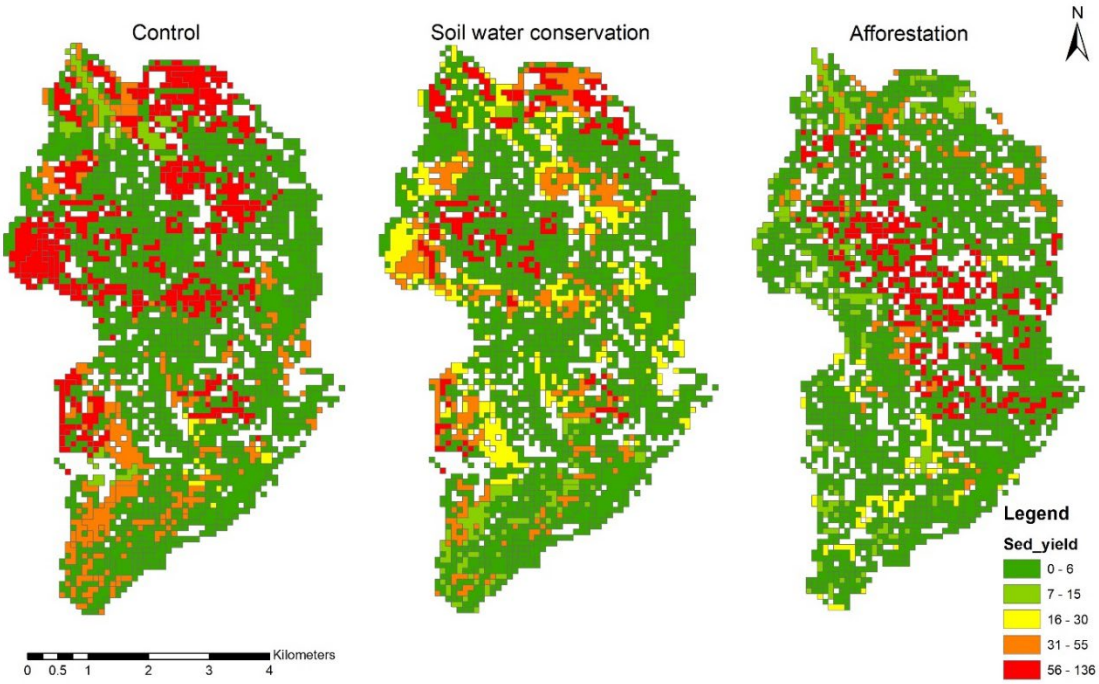

Figure 14. The long-term (1990-2019) mean annual sediment yields in t ha^{-1} y^{-1} per HRU for the control, control with improved SWC practices and afforestation scenario.

As the results on subbasin level have shown; the land use did have an impact on the soil erosion in the watershed. In order to evaluate this impact the sediment yields per HRU and land use were determined. At HRU level, the sediment yields are in a range between 0 and 136 t ha^{-1} y^{-1} (figure 14). The sediment yields for HRUs with *A. decurrens* have a max. of 7.9 t ha^{-1} y^{-1},

HRUs with pastures 0.6 t ha^{-1} y^{-1} and HRUs with forests 0.3 t ha^{-1} y^{-1}. Be that as it may cropland had sediment yields ranging between 0.5 and 136 t ha^{-1} y^{-1}. Also good to keep in mind is that for all land uses the sediment yield increased as the slope inclined (table 11).

Table 10. Mean annual sediment yield in t ha^{-1} y^{-1} per subbasin for the control, control with improved SWC practices and afforestation scenario and the reduction in sediment for the control with improved SWC practices and afforestation scenario in comparison with the control.

Subbasins	Mean annual sediment yield (t ha^{-1} y^{-1})						Reduction in sediment yield (%)	
	Control		SWC		Afforestation		2002	2019
	Mean	STD	Mean	STD	Mean	STD	SWC	Afforestation
1	47.8	23.1	33.6	16.1	12.1	5.6	-29.7	-74.8
2	52.7	25.0	32.6	15.2	23.7	11.4	-38.2	-55.1
3	87.4	41.3	59.8	28.2	8.1	5.5	-31.5	-90.7
4	5.0	2.1	2.8	1.2	26.0	12.1	-44.5	422.9
5	26.4	12.1	13.2	6.1	7.7	3.5	-49.9	-70.8
6	44.5	20.7	18.8	8.7	11.8	5.4	-57.7	-73.4
7	15.3	7.0	12.1	5.6	10.7	4.8	-20.9	-30.1
8	3.9	1.7	1.9	0.9	11.2	5.6	-51.7	187.4
9	43.4	20.0	35.5	16.3	42.1	19.0	-18.2	-3.0
10	54.6	24.2	22.1	10.0	4.9	2.2	-59.4	-91.0
11	20.1	9.1	16.2	7.4	50.5	22.4	-19.3	150.6
12	50.2	22.2	21.5	9.7	3.2	2.5	-57.3	-93.5
13	3.2	1.4	1.6	0.7	3.9	1.7	-50.6	20.1
14	4.0	1.8	1.9	0.9	14.1	6.2	-53.0	251.2
15	28.6	12.7	11.9	5.4	53.0	23.1	-58.4	85.1
16	49.5	21.9	26.2	11.9	4.4	1.9	-47.0	-91.0
17	0.0	0.0	0.0	0.0	0.1	0.1	0.0	651.9
18	6.3	2.8	2.4	1.1	27.0	11.8	-61.8	325.8
19	54.1	24.9	29.9	13.7	4.7	2.6	-44.8	-91.3
20	8.5	4.0	3.3	1.5	13.7	6.5	-61.8	60.5
21	11.5	5.3	4.4	2.0	12.9	6.1	-61.9	12.4
22	1.6	0.8	0.7	0.3	3.0	1.4	-54.9	85.6
23	38.1	17.4	22.6	10.4	25.3	11.5	-40.6	-33.6
24	7.0	3.1	4.5	2.0	5.4	2.4	-34.6	-21.8
25	19.4	8.4	9.4	4.2	2.2	1.1	-51.3	-88.5
26	5.7	3.0	4.1	2.2	7.0	3.6	-28.5	22.9
27	12.9	6.5	8.4	4.3	5.4	2.6	-35.3	-58.5

In figure 14 there is a clear shift visible from erosion hotspot between the control and the afforestation practice. The areas with high erosion in the control have changed to some extent from cropland to *A. decurrens* plantations and pasture. However, in the centre of the watershed

cropland was extended in some area resulting in a shift of soil erosion hotspots. In the afforestation scenario, the hotspots are areas with cropland and they have mainly a slope of ≥20%.

The HRUs with *A. decurrens* were having a higher sediment yield than the forest land use. The sediment yields would have been similar to the forest land use if not for the fact that during the first year of the agroforestry rotation the *A. decurrens* seedlings are intercropped with teff. Consequently, during the first year the sediment yields were similar to those of cropland. Even when not intercropped with teff, a higher soil erosion would be expected due to the bare soil during this stage. The other years the forest and *A. decurrens* land uses had roughly the same sediment yields. For the *A. decurrens*, excluding the first year of the cycle, the mean sediment yield ranged from 0.03 – 0.20 t ha^{-1} y^{-1}, which was close to the range of the forest land use of 0.02 – 0.20 t ha^{-1} y^{-1}.

Comparing the sediment yields with the soil loss that the SWAT model calculated, there are some differences. On average the soil loss is 2 t ha^{-1} y^{-1} higher than the sediment yields. For the plantations the soil loss is 1-2 t ha^{-1} y^{-1} higher and for the cropland 0.5-15 t ha^{-1} y^{-1}. However, for pastures and forest land use the values are rather similar. In appendix C, the soil loss per land use and slope class.

Table 11. Mean annual sediment yield in t ha^{-1} y^{-1} for the different land uses and slopes for the control, SWC and afforestation scenarios. ADEC; A. decurrens, FRST; forest, PAST; pasture, TEFF; teff.

Land use	Slope	Annual sediment yield (t ha^{-1} yr^{-1})					
		Control	SWC	Afforestation	Control	SWC	Afforestation
		Mean			STD		
ADEC	0 - 5	-		0.9	-		-
ADEC	5 - 12	-		1.5	-		0.13
ADEC	12 - 20	-		2.5	-		0.19
ADEC	20 – 30	-		2.8	-		0.23
ADEC	> 30	-		3	-		-
FRST	0 – 5	0.01		0.02	0.003		0.0005
FRST	5 - 12	0.07		0.07	0.02		0.0002
FRST	12-20	0.1		0.1	0.02		0.0008
FRST	20 – 30	0.2		0.2	0.02		0.002
FRST	> 30	-		0.2	-		0.004
PAST	0 - 5	0.05		0.06	0.03		0.001
PAST	5 - 12	0.2		0.2	0.07		0.004
PAST	12-20	0.3		0.3	0.1		0.01
PAST	20 – 30	0.5		0.5	0.2		0.01
TEFF	0 - 5	1.3	0.9	7.1	4.6	1.7	0.5
TEFF	5 - 12	29.5	10.4	23.6	24.5	8.5	1.9
TEFF	12-20	38.6	17.9	33.5	36.8	16.9	2.7
TEFF	20 – 30	75.5	63.6	59.4	48.8	41.0	3.9

5. Discussion

The water balance partitioning did show some unexpected changes with the implementation of afforestation practices in this study. The results have shown that it is more than likely that crop parameters of the *A. decurrens* have impacted the water balance. In this discussion a comparison of results with other studies, data limitations and model errors and steps to further develop the SWAT model.

5.1. Comparison of results with other studies

Comparing the land use change from an annual cropping to an afforestation system in the watershed with the overall land use change in the Fagita Lekoma District there are some similarities. In the watershed there is an annual increase of cultivated and natural forest of 19%, Belayneh et al. reported a similar increase of 18% for the district. The cropland in the watershed reduced between 2002 and 2019 annually with 2%. Wondie and Mekuria (2018) reported an annual decrease in cropland of 2% (2000-2010) and of 1% (2010-2015) and Belayneh *et al.* (2018) reported an annual decrease of 2% (2003 - 2017). Neither Belayneh *et al.* or Wondie and Mekuria reported a decrease in the district of grassland while in the watershed there is an annual decrease of approximately 4%.

The effects of afforestation on water availability is contested by scientist, since trees use a lot of water. The afforestation practices in arid regions in China could potentially lead to water scarcity, reduced runoff and a drier climate (Zastrow 2019). According to Zethof *et al.* (2019) water availability in the semiarid regions of Spain might be enhanced by better infiltration of rainwater through preferential flow paths. Studies in different countries mention the improvement of soil quality and reduction of erosion as an important reason to implement afforestation practices (Ilstedt *et al.* 2007; Nadal-Romero *et al.* 2016). Several studies have been conducted on the hydrology of the Upper Blue Nile Basin, however there is a focus on impacts of e.g. SWC practices or climate change on the streamflow and runoff on catchment scale (Dile *et al.* 2013a; Lemann *et al.* 2017; Melaku *et al.* 2018) or soil erosion and runoff on plot scale (Dagnew *et al.* 2015; Ebabu *et al.* 2018). However, there are no estimates of the impact of the afforestation practices on the landscape water balance.

Ilstedt *et al.* (2007) touched on the fact that studies suggest that afforestation increased the infiltrability in tropical soils. Knowledge on impacts of species, techniques and also the infiltration rates is severely lacking and there is only a limited amount of studies conducted on soil physical properties.

Tadesse (2020) assessed the infiltration rates under different land use practices at four sites in the studied watershed. The *A. decurrens* plantations had the highest infiltration rates followed by cropland and grazing land and this did not significantly differ between sites except for the infiltration at four year old *A. decurrens* plantations. Improved bulk density and organic carbon in the *A. decurrens* plantations potentially resulted in higher infiltration rates. These results can however not be scaled up from plot to landscape scale in the watershed, since so many factors influence the infiltration rates and they can be site specific. With the SWAT model the percolation is simulated and not the infiltration. The percolation is the water flux that passes the bottom boundary of the soil profile into the saturated zone. While infiltration is the water entering the soil from the soil surface. The percolation in this study is highest for the *A. decurrens* and forest land uses. Cropland and pasture land uses both had a lower percolation rate. These results are in line with measurements by Tadesse (2020). However, since there was a lower ET_a this could have resulted in higher percolation rates for the afforestation scenario with a maximum rate of 7 mm d^{-1}. The infiltration rate, although not measured, is higher than the percolation rate and in the model it was assumed there is no surface sealing taking place and that there is no dynamic soil structure that would account for the improved soil quality.

Abtew and Dessu (2019b) referred that land use and land management change in the Upper Blue Nile Basin could potentially reduce the flow in the Blue Nile. A lower streamflow and baseflow coming from upstream can have a severe impacts on areas further downstream. Based on this SWAT simulation the streamflow is not reduced but slightly increased for the afforestation scenario in comparison with the control. Also the baseflow seems to be steadier during the year in the afforestation scenario.

According to Abera *et al*. (2020) soil loss for Ethiopia is ranging from 3.4 till 84.5 t ha^{-1} y^{-1} with a max. rates of 300 t ha^{-1} y^{-1}. In the studied watershed, the overall sediment yields that were simulated ranged from 15.3 till 26.5 t ha^{-1} y^{-1} and were within the range of Abera *et al*. (2020). The soil loss, calculated in SWAT for comparison reasons, was approximately 2 t ha^{-1} y^{-1} higher than the sediment yields, still well within the range of Abera *et al.* (2020).

The soil loss in Ethiopia was found to be highest for cropland, ranging from 50 to 179 t ha^{-1} y^{-1} (Abera *et al.* 2020). The higher soil erosion rates for cropland in this study were also in line with Abera *et al.* (2020). Land cultivated with teff, dependent on the slope, had mean soil erosion rates ranging from 1 to 84 t ha^{-1} y^{-1}. There were maximums simulated over a 30 year period of 114, 121 and 136 t ha^{-1} y^{-1}.

The effect of biological interventions on plot level, such as afforestation and grass strips, have a mean effect size of -90% to -68% on soil erosion and -48% to -21% on runoff (Abera et al. 2020). Also a significant reduction of soil erosion and runoff is mentioned for terraces. Although this study was not conducted on plot level, at subbasin level there are reductions visible between the control and the other two scenarios. There were reductions of sediment yield ranging between 18% and 62% for the control with improved SWC practices. For the afforestation scenario the reduction was specific per subbasin but reductions between 3% and 94% were simulated.

The impact of climate change on water balance partitioning was beyond the scope of this study. Nevertheless, there are concerns by countries in the Nile Basin on potential changes in

the river discharge and adaption strategies implemented in upstream areas. Several studies have been done on the impact of climate change on the discharge of the Blue Nile. The results of these studies are highly variable and often the effects of (future) land use change were not taken into account (Tesemma *et al.* 2010).

5.2. Data limitations, model errors and next steps

Input data limitations

For the watershed there is at the moment little empirical data available. Empirical data and ground truthing of this watershed is currently still under way. The input data was collected from different sources and there were limitations when it came to resolution, validation and ground truthing of the data. The watershed is only 32 km^2 and some of the input data was coarse for a watershed of this size.

The DEM used in this study had a resolution of 90 m (Jarvis *et al.* 2008). This resulted in, when modelling the watershed, that the land use and soil maps were both transformed to a resolution of 90 meter. For further development of the model a DEM with a resolution of 10 or 30 meters should be used to improve the resolution of land use and soil data in SWAT. The stream network that was created for the watershed was for this study burned in. The burn in function defines the location of the stream network in SWAT (Luo *et al.* 2011). Defining the stream network without the burned in function resulted in a coarse stream network in the watershed. With a higher resolution DEM, a better representation of the stream network is expected as well.

The WRB soil map (Hengl *et al.* 2017) used in SWAT is homogeneous for the watershed and the surrounding area. Because of this the SWAT program assumed there is in the watershed only one soil type; Nitisols. The soil physical properties were only altered on subbasin level, which was done based on the soil maps (Hengl *et al.* 2015). However, based on the soil maps there were within subbasins variations, e.g. bulk density, organic carbon and clay content. Creating a more detailed soil map to account for these variations would be a possibility to improve the soil data in the model. Also, changes for different land uses could be made for the soil physical properties, this to also further improve the soil data in the model. The depth of the soil profile was defined in the study to be 2 meters. There are however areas in the watershed where the soil profile would probably be shallower or considerably deeper. Adapting the soil depths in slope and lowland areas in the watershed should also be considered to better represent the soil profile in the watershed. The available water capacity (AWC) and saturated hydraulic conductivity (K_{sat}) were determined based on coarse maps (250m and 1000m resolution) and limited literary sources. Both parameters are important for the water holding capacity in the soil. Measuring the field capacity and permanent wilting point on samples taken in the watershed is highly recommended to determine the AWC. Also the K_{sat} will need to be revisited, field or lab measurements can be used to calculate the K_{sat}.

The parameters for the *A. decurrens* were determined based on literature research. Several studies mention the height, diameter at breast height (DBH) and wood and foliage biomass, see

appendix D (Kindu *et al.* 2006; Mekonnen *et al.* 2006; Ferede *et al.* 2019; Amha *et al.* 2020). However, for the *A. decurrens* there is little work done on the effects of water stress, nutrient uptake, root depth, root distribution and growth response. For parameters like the leaf area index (LAI) and radiation efficiency (RUE) values from the *Acacia mearnsii* were used. Although the two trees are similar there could have been an over- or underestimation of values. To improve the crop parameters field verification needs to be done on the growth response parameters and water and nutrient uptake parameters.

SWAT model calibration and validation

During this study, the SWAT model was not calibrated and validated, despite that it is an essential part of the modelling (Arnold *et al.* 2012b). Model calibration and validation can be done by comparing model predictions with observed data and better parameterize the model (calibration) and eventually comparing the calibrated model predictions with observed data (validation). Because of a limited amount of empirical data this could not be done at this time. The calibration and validation are important steps in the further development of the model.

Due to limited availability of empirical data for the watershed another way of calibration and validation is needed. If there is streamflow data available for the watershed this can be used to calibrate and validate the model (Dile *et al.* 2013a; Lemann *et al.* 2017). Nevertheless, (long term) streamflow data might not be available on the watershed. Remotely sensed data to derive i.e. the evapotranspiration can be used as an alternative for the calibration and validation of the model because of the limited available hydrological data (Senkondo *et al.* 2019). Long-term data needs to be collected to be able to derive the ET_a and to have a considerable validation and calibration time. Senkondo et al. (2019) used satellite images, i.e. emissivity, normalized difference vegetation index and albedo, of the moderate resolution imaging spectroradiometer (MODIS) to derive the ET_a. There are several models that can be used to derive the required ET_a data e.g. surface energy balance models, surface balance algorithm for land model or operational simplified surface energy balance model (Senkondo 2020). The change of land use can alter the ET_a and data should be used with some caution.

Change from annual cropping to afforestation in 17 years

The land use classification was done based on satellite images (Google Earth *et al.* 2002; Google Earth & CNES / Airbus 2019; ESRI *et al.* 2020). To make sure as little area was over- or underestimated, both Google Earth and Landsat images with agriculture and vegetation rendering were used. Maps created were compared carefully with the original satellite images after land use classification. The intercropped *A. decurrens* seedlings could possibly have been classified as cropland. Also, fields where the *A. decurrens* has just been harvested and charcoal has been made on the fields, might in some cases have been classified as cropland or pasture, this due to the colouring of the fields. On the land use map of 2002 there are no buildings classified, while in 2019 buildings are classified. There is a clear change visible in the roofs between 2002 and 2019, where in 2002 there were mainly grass thatched roofs and in 2019 there are corrugated roofs. The corrugated roofs were classified as buildings while the grass thatched roofs were classified as either cropland or pasture. The mild cloud cover on the 2002

satellite images might also have resulted in some minor errors in the land use classification. During this study the use of a map with minor cloud cover was chosen because maps without were having a much lower resolution and were not available of the growing season. Overall the certainty can be improved by creating a wider set of land use maps and closely comparing them with satellite images and by doing further analysis with ArcMap.

In SWAT the land use was slightly altered by the program when creating HRUs, see table 12 for the altered values. In SWAT the certainty can be improved by making sure there is a higher resolution DEM and to change the threshold values.

Table 12. HRU land cover for 2002 and 2019 and the changes between the land class classification (LCC) and the HRU.

Land cover	2002			2019		
	Area (ha)	Area (%)	LCC and HRU change (%)	Area (ha)	Area (%)	LCC and HRU change (%)
Pasture	1,058	33	2.4	215	7	-46.2
Teff	1,913	61	7.3	1,504	48	15.4
Forest	190	6	-44.8	336	11	-31.5
Acacia decurrens	-	-	-	1,106	35	14.4
Urban	-	-	-	1	0.03	N/A

Rainfall characteristics

MERRA-2 global atmospheric reanalysis datasets ((NASA 2018) were used to obtain the required climate data. The grid points that represent the stations were located outside the watershed. A t-test ran on the datasets and showed no significant difference between the two datasets. There are some limitations when it comes to the use of the MERRA-2 data.

The grid points were located at an elevation of 1,864 and 1,839 meter, at some distance from the watershed. However the watershed is located at an elevation of 2,390 to 2,915 meter. The high topography can cause problems in MERRA-2 which could result in excessive precipitation in these areas (Gelaro *et al.* 2017). MERRA-2 is corrected with local observations to improve the data quality (Gelaro *et al.* 2017). The highlands of Ethiopia are a data scarce area in terms of observed continuous data. Meteorological stations are spread irregularly and the data is missing from time to time. Preferably one or more meteorological stations in the watershed would be helpful to account for the rainfall variability and patterns at this altitude.

The second point is that the importing of the data into SWAT can cause additional errors. The precipitation in the watershed was based on the two grid point that were used by SWAT to determine the regional precipitation. Only a fraction of the true precipitation is in this way captured (S.L. Neitsch *et al.* 2011). Any regional variations in precipitation are because of the limited data around the watershed not captured.

Actual evapotranspiration

The ET_a for the *A. decurrens*, based on the simulation results, was in comparison with the other land uses low (table 13). The STD of the ET_a for the *A. decurrens* was higher which would indicate a higher variation. An ET_a similar to the forest land use was expected for the *A. decurrens*. The ET_a of the *A. decurrens* also varies during the different stages of the agroforestry cycle.

Table 13. Mean and standard deviation of the actual evapotranspiration for the afforestation land uses.

	A. decurrens	Forest	Teff	Pasture
Annual mean (mm y^{-1})	567	791	910	1,126
Standard deviation (mm y^{-1})	229	60	83	99

The aforementioned crop parameters for the *A. decurrens* are based on literature (Appendix B). To optimize the ET_a the crop parameters should first be re-evaluated. The LAI and stomatal conductance of water vapour are two parameters that have an impact of the ET_a. Three parameters are needed to model the stomatal conductance in SWAT; the maximum stomatal conductance at high solar radiation and low vapour pressure deficit (m s^{-1}), the vapour pressure deficit (kPa) and the fraction of maximum stomatal conductance (-) (Arnold *et al.* 2012a). The parameters were defined as 0.0036 m s^{-1}, 4 kPa and 0.75. The stomatal conductance is for most trees either 0.0036 or 0.007 m s^{-1}. The maximum potential leaf area index (BLAI) was defined as 3.5. Comparing the predefined forest land use the BLAI is for most trees between 2 and 5. By adapting the stomatal conductance to 0.007 m s^{-1} and the BLAI to 5 the annual mean ET_a was increased from 567 to 725 mm y^{-1} (STD of 189 mm y^{-1}).

The roots are another sensitive parameter that can impact the ET_a. For the *A. decurrens,* the maximum root depth was set to 1 meter due to the shallow root system mentioned in literature. Water is taken up by the roots and transpired. Potentially the roots of the *A. decurrens* were not deep enough in the model to have access to the required amount of water. The *A. decurrens* in the model also went into dormancy for 10 days. This resulted into a loss of leaf biomass and a drop in ET_a at the end of the year. The trees were not expected to go into dormancy, although some loss of leaf biomass was expected through the year. In the model, the leaf biomass was decomposed and resulted in an increase of C and N.

Overall it is important that the growth response parameters and root depth of the *A. decurrens* are correct because the water balance is sensitive when it comes to these parameters. It is likely that in this study the *A. decurrens* description has affected the water balance. Therefore, the next steps would be to have field verification of parameters related to the leaf area index, biomass-energy ratio and stomatal conductance. Verification should be done at different development stages and preferably during different seasons.

The impact of land use change on the sediment yield

For future reference, the surface runoff that is an important part of the generation of soil erosion, needs to be evaluated. The surface runoff on the *A. decurrens* plantations is higher than expected (table 14). Due to the high LAI, the expectation was that a part of precipitation would be intercepted the canopy of the *A. decurrens* and as a result less runoff would be created. For

the teff and pasture land uses a small decrease is visible, this could be dependent on the slope and the area. However this cannot be stated with certainty.

The CN value was in this study adapted from 87 to 79 to reduce the runoff, this was done to have a similar CN value as the forest land use. During further development of the model a close look will have to be taken at the aforementioned crop parameters and surface runoff components.

Also, SWC practices, in the form of terraces and contouring, will need to be implemented in the afforestation model. Farmers use these practices in the watershed to reduce surface runoff and limit soil erosion. These practices can be implemented in the afforestation model in the same way as was done for the control with improved SWC practices by altering the CN values, USLE P factor and slope lengths.

Table 14. Mean surface runoff in mm day^{-1} for the four different land uses of the control and afforestation scenario.

	Acacia decurrens	Forest	Teff	Pasture
Control	-	1.6	1.9	1.6
Afforestation	1.8	1.6	1.8	1.5

6. Conclusion

This study was aimed to explore the impact of agricultural land use change on a landscape water balance. The modelling resulted in some unexpected changes between the control and afforestation scenario. The key research questions have led to these results in this study:

1. The agricultural land use in the watershed in the Fagita Lekoma District has changed over the last 17 years. The watershed was dominated by cropland and pastures in 2002 and there was only a limited amount of forest left in the watershed. In 2019 the land use has changed in the watershed, cropland is still dominating but next to annual crops the *A. decurrens* plantations are dominating.
2. Minor changes in the water balance partitioning were visible between the control and the afforestation land use. In the modelling a higher ET_a and a lower surface runoff were expected due to a high biomass density in the *A. decurrens* plantations. The percolation and subsequently the groundwater flow in the watershed increased significantly in the afforestation land use but could have been an effect of the lower ET_a. Despite the land use change there does not seem to be a significant difference for most of the water balance components.
3. For the field scale soil and water conservation practices in the form of terraces, there were in essence no significant changes in the water balance. The surface runoff was reduced and also a minor increase in percolation and groundwater flow could be observed but they were not significant.
4. The impact of land use change on the sediment yields has led to a reduction in both the control with improved SWC practices and the afforestation scenario. Targeting the cropland with SWC practices resulted in a reduction in sediment yield. For the afforestation land use the same thing can be said but areas with cropland remain prone to soil erosion.
5. The growth response parameters designed for the *A. decurrens* have shown to be sensitive and they have more than likely impacted the water balance in this study. Therefore, next steps should be field verification of growth response parameters and water and nutrient uptake parameters. Furthermore, to support calibration and validation of the model higher resolution input data needs to be acquired.

Acknowledgements

I am extremely grateful to my supervisor Jennie Barron for her unwavering support, helpful advice and invaluable insight into the watershed. I am also grateful to Erik Karltun for his insightful suggestions and knowledge on the watershed and the agroforestry practices. Many thanks to those whom have helped solve the problems I faced with ArcGIS and SWAT during the course of this project.

This work is related to the project Market driven afforestation – trajectories in social resilience and environmental sustainability under land-use intensification led by SLU in partnership with University of Gonder and Wondo Genet College of Forestry and Natural Resources, Hawassa University.

References

Abdelkadir, A. & Yimer, F. (2011). Soil water property variations in three adjacent land use types in the Rift Valley area of Ethiopia. *Journal of Arid Environments*, vol. 75 (11), pp. 1067–1071

Abera, W., Tamene, L., Tibebe, D., Adimassu, Z., Kassa, H., Hailu, H., Mekonnen, K., Desta, G., Sommer, R. & Verchot, L. (2020). Characterizing and evaluating the impacts of national land restoration initiatives on ecosystem services in Ethiopia. *Land Degradation & Development*, vol. 31 (1), pp. 37–52

Abtew, W. & Dessu, S.B. (2019a). Grand Ethiopian Renaissance Dam Reservoir Filling. In: Abtew, W. & Dessu, S.B. (eds.) *The Grand Ethiopian Renaissance Dam on the Blue Nile*. Cham: Springer International Publishing, pp. 97–113.

Abtew, W. & Dessu, S.B. (2019b). Introduction. In: Abtew, W. & Dessu, S.B. (eds.) *The Grand Ethiopian Renaissance Dam on the Blue Nile*. Cham: Springer International Publishing, pp. 1–11.

Adimassu, Z., Langan, S. & Barron, J. (2018). *Highlights of soil and water conservation investments in four regions of Ethiopia*. International Water Management Institute (IWMI). DOI: https://doi.org/10.5337/2018.214

Africa Soil Information Service (AfSIS) (2015). *Africa Soil Profile Database*. *Africa Soil Information Service*. Available at: http://africasoils.net/services/data/soil-databases/africa-soil-profile-database/

Allam, M.M., Figueroa, A.J., McLaughlin, D.B. & Eltahir, E.A.B. (2016). Estimation of evaporation over the upper Blue Nile basin by combining observations from satellites and river flow gauges. *Water Resources Research*, vol. 52 (2), pp. 644–659

Allen, R.G., Pereira, L.S., Raes, D. & Smith, M. (1998). *Crop evapotranspiration - guidelines for computing crop water requirements*. (56). Rome, Italy: FAO.

Amha, Y., Tesfaye, M.A., Kassa, Z. & Argaw, M. (2020). Growth and biomass production of some selected native and introduced tree/shrub species under severely degraded landscapes of west showa zone of oromiya regional state, central highlands of Ethiopia. *Forestry Research and Engineering: International Journal*, vol. 4 (1), pp. 28–34

Arnold, J.G., Kiniry, J.R., Srininvasan, R., Williams, J.R., Haney, E.B. & Neitsch, S.L. (2012a). Soil and Water Assessment Tool, Input/Output Documentation Version 2012. Texas Water Resource Institute.

Arnold, J.G., Moriasi, D.N., Gassman, P.W., Abbaspour, K.C. & White, M.J. (2012b). SWAT: Model use, calibration, and validation. *Soil and Water Division of ASABE*, vol. 55 (4), p. 20

Asadi Zarch, M.A., Sivakumar, B. & Sharma, A. (2015). Droughts in a warming climate: A global assessment of Standardized precipitation index (SPI) and Reconnaissance drought index (RDI). *Journal of Hydrology*, vol. 526, pp. 183–195 (Drought processes, modeling, and mitigation)

Asmamaw, L.B. & Mohammed, A.A. (2013). Effects of slope gradient and changes in land use/cover on selected soil physico-biochemical properties of the Gerado catchment, north-eastern Ethiopia. *International Journal of Environmental Studies*, vol. 70 (1), pp. 111–125 Routledge.

Asmare, M.T. & Gure, A. (2019). Potential of exclosure on aboveground biomass carbon stock and ecological fitness of woody species in Jabi Tehnane district, northwestern Ethiopia. *Ecosystem Health and Sustainability*, vol. 5 (1), pp. 79–85 Taylor & Francis.

Ayele, M., Blum, A. & Nguyen, H.T. (2001). Diversity for osmotic adjustment and root depth in TEF [Eragrostis tef (Zucc) Trotter]. *Euphytica*, vol. 121, pp. 237–249

Bayabil, H.K., Dile, Y.T., Tebebu, T.Y., Engda, T.A. & Steenhuis, T.S. (2019). Evaluating infiltration models and pedotransfer functions: Implications for hydrologic modeling. *Geoderma*, vol. 338, pp. 159–169

Bazie, Z., Feyssa, S. & Amare, T. (2020). Effects of Acacia decurrens Willd. tree-based farming system on soil quality in Guder watershed, North Western highlands of Ethiopia. *Cogent Food & Agriculture*, vol. 6 (1), p. 1743622 Cogent OA.

Bekele, T.A. (2007). *Useful trees and shrubs for Ethiopia: identification, propagation and management for 17 agroclimatic zones*. Nairobi Kenya: World Agroforestry Centre. Available at: http://www.worldagroforestry.org/publication/useful-trees-and-shrubs-ethiopia-identification-propagation-and-management-17 [2020-03-07]

Belayneh, Y., Guo, R., Alemu, A., Lakew, Z. & Mengesha, T. (2018). Forest cover change and its driving forces in Fagita Lekoma District, Ethiopia. *Journal of Forestry Research*,

Berhanu, B., Seleshi, Y. & Melesse, A.M. (2014). Surface Water and Groundwater Resources of Ethiopia: Potentials and Challenges of Water Resources Development. In: Melesse, A.M., Abtew, W., & Setegn, S.G. (eds.) *Nile River Basin: Ecohydrological Challenges, Climate Change and Hydropolitics*. Cham: Springer International Publishing, pp. 97–117.

Berihun, M.L., Tsunekawa, A., Haregeweyn, N., Meshesha, D.T., Adgo, E., Tsubo, M., Masunaga, T., Fenta, A.A., Sultan, D. & Yibeltal, M. (2019). Exploring land use/land cover changes, drivers and their implications in contrasting agro-ecological environments of Ethiopia. *Land Use Policy*, vol. 87, p. 104052

Bewket, W. & Teferi, E. (2009). Assessment of soil erosion hazard and prioritization for treatment at the watershed level: Case study in the Chemoga watershed, Blue Nile basin, Ethiopia. *Land Degradation & Development*, vol. 20 (6), pp. 609–622

Birhanu, A. (2014). Environmental Degradation and Management in Ethiopian Highlands: Review of Lessons Learned., 2014.

Bulcock, H.H. & Jewitt, G.P.W. (2010). Spatial mapping of leaf area index using hyperspectral remote sensing for hydrological applications with a particular focus on canopy interception. *Hydrology and Earth System Sciences*, vol. 14 (2), pp. 383–392 Copernicus Publications.

Clulow, A.D., Everson, C.S. & Gush, M.B. (2011). *The Long-term impact of acacia mearnsii trees on evaporation, streamflow and groundwater resources*. (TT505/11). Water Research Commision.

Corral-Pazos-de-Provens, E., Domingo-Santos, J.M. & Rapp-Arrarás, Í. (2018). Estimating the very fine sand fraction for calculating the soil erodibility K-factor. *Land Degradation & Development*, vol. 29 (10), pp. 3595–3606

Dagnew, D.C., Guzman, C.D., Zegeye, A.D., Tibebu, T.Y., Getaneh, M., Abate, S., Zemale, F.A., Ayana, E.K., Tilahun, S.A. & Steenhuis, T.S. (2015). Impact of conservation practices on runoff and soil loss in the sub-humid Ethiopian Highlands: The Debre Mawi watershed. *Journal of Hydrology and Hydromechanics*, vol. 63 (3), pp. 210–219

Dereje Ayalew (2012). Variability of rainfall and its current trend in Amhara region, Ethiopia. *AFRICAN JOURNAL OF AGRICULTURAL RESEEARCH*, vol. 7 (10). DOI: https://doi.org/10.5897/AJAR11.698

Dile, Y.T., Berndtsson, R. & Setegn, S.G. (2013a). Hydrological Response to Climate Change for Gilgel Abay River, in the Lake Tana Basin - Upper Blue Nile Basin of Ethiopia. *PLOS ONE*, vol. 8 (10), p. e79296 Public Library of Science.

Dile, Y.T., Karlberg, L., Daggupati, P., Srinivasan, R., Wiberg, D. & Rockström, J. (2016). Assessing the implications of water harvesting intensification on upstream–downstream ecosystem services: A case study in the Lake Tana basin. *Science of The Total Environment*, vol. 542, pp. 22–35

Dile, Y.T., Karlberg, L., Temesgen, M. & Rockström, J. (2013b). The role of water harvesting to achieve sustainable agricultural intensification and resilience against water related shocks in sub-Saharan Africa. *Agriculture, Ecosystems & Environment*, vol. 181, pp. 69–79

Dile, Y.T., Tekleab, S., Ayana, E.K., Gebrehiwot, S.G., Worqlul, A.W., Bayabil, H.K., Yimam, Y.T., Tilahun, S.A., Daggupati, P., Karlberg, L. & Srinivasan, R. (2018). Advances in water resources research in the Upper Blue Nile basin and the way forward: A review. *Journal of Hydrology*, vol. 560, pp. 407–423

DSA & SCI (2005). *Potential survey, identification of opportunities and preparations of projects profiles and feasibility studies. Part one: potential assessment survey*

Dye, P. & Jarmain, C. (2004). Water use by black wattle (Acacia mearnsii) : implications for the link between removal of invading trees and catchment streamflow response : working for water. *South African Journal of Science*, vol. 100 (1–2), pp. 40–44 Academy of Science for South Africa (ASSAf).

Ebabu, K., Tsunekawa, A., Haregeweyn, N., Adgo, E., Meshesha, D.T., Aklog, D., Masunaga, T., Tsubo, M., Sultan, D., Fenta, A.A. & Yibeltal, M. (2018). Analyzing the variability of sediment yield: A case study from paired watersheds in the Upper Blue Nile basin, Ethiopia. *Geomorphology*, vol. 303, pp. 446–455

Elkollaly, M., Khadr, M. & Zeidan, B. (2018). Drought analysis in the Eastern Nile basin using the standardized precipitation index. *Environmental Science and Pollution Research*, vol. 25 (31), pp. 30772–30786

Elsanabary, M.H. & Gan, T.Y. (2015). Evaluation of climate anomalies impacts on the Upper Blue Nile Basin in Ethiopia using a distributed and a lumped hydrologic model. *Journal of Hydrology*, vol. 530, pp. 225–240

Endalamaw, B. (2019). Developing A Form Factor Function for Acacia Decurrensin Southwestern Amhara National Regional State, Ethiopia. *Berhan International Research Journal of Science and Humanities*, vol. 3 (1), pp. 126–138

Esa, E., Assen, M. & Legass, A. (2018). Implications of land use/cover dynamics on soil erosion potential of agricultural watershed, northwestern highlands of Ethiopia. *Environmental Systems Research*, vol. 7 (1), p. 21

ESRI, USGS & METI/NASA (2020). *Landsat explorer*. *Landsat explorer*. Available at: https://livingatlas2.arcgis.com/landsatexplorer/

Essenfelder, A.H. (2018). *SWAT weather database*. Version: v.0.18.03.

Ethiopian Agricultural Transformation Agency EthioSIS. *ATA*. Available at: http://www.ata.gov.et/programs/highlighted-deliverables/ethiosis/ [2020-06-24]

Ethiopian mapping agency (EMA) (1987a). Adis Kidame 1136 D4 1 EMA 1987. Topographic map, Ethiopian mapping agency (EMA). ETH 4

Ethiopian mapping agency (EMA) (1987b). Gimja Bet 1036 B2 1 EMA 1987. Topographic map, Ethiopian mapping agency (EMA). ETH 4

Ethiopian National Meteorology Agency *Climate of City: Bahir Dar*. *NMA national meteorology agency*. Available at: http://www.ethiomet.gov.et/climates/climate_of_city/2648/Bahir%20Dar

FAO (2016). *AQUASTAT Country Profile*. Rome, Italy: Food and Agriculture Organization of the United Nations (FAO).

FAO (2020). *Ethiopia at a glance | FAO in Ethiopia | Food and Agriculture Organization of the United Nations*. Available at: http://www.fao.org/ethiopia/fao-in-ethiopia/ethiopia-at-a-glance/en/ [2020-05-21]

FAO, IIASA, ISRIC, ISSCAS & JRC (2012). *Harmonized World Soil Database (version 1.2)*. FAO, Rome, Italy and IIASA, Laxenburg, Austria.

Ferede, T., Alemu, A. & Mariam, Y.G. (2019). Growth, Productivity and Charcoal Conversion Efficiency of Acacia decurrens Woodlot. *Journal of Academia and Industrial Research (JAIR)*, vol. 8 (6), p. 8

Gebrehiwot, S.G., Ilstedt, U., Gärdenas, A.I. & Bishop, K. (2011). Hydrological characterization of watersheds in the Blue Nile Basin, Ethiopia. *Hydrology and Earth System Sciences*, vol. 15 (1), pp. 11–20

Gelaro, R., McCarty, W., Suárez, M.J., Todling, R., Molod, A., Takacs, L., Randles, C.A., Darmenov, A., Bosilovich, M.G., Reichle, R., Wargan, K., Coy, L., Cullather, R., Draper, C., Akella, S., Buchard, V., Conaty, A., da Silva, A.M., Gu, W., Kim, G.-K., Koster, R., Lucchesi, R., Merkova, D., Nielsen, J.E., Partyka, G., Pawson, S., Putman, W., Rienecker, M., Schubert, S.D., Sienkiewicz, M. & Zhao, B. (2017). The Modern-

Era Retrospective Analysis for Research and Applications, Version 2 (MERRA-2). *Journal of Climate*, vol. 30 (14), pp. 5419–5454 American Meteorological Society.
Google Earth & CNES / Airbus (2017). *Satellite map Fagta Lekoma 16 december 2017, 11° 1'17.73"N, 36°52'52.14"E, elevation 2400-2900m*. Version: 7.3.2.5776 (64-bit).
Google Earth & CNES / Airbus (2019). *Satellite map Fagta Lekoma 28 December 2019, 11° 1'17.73"N, 36°52'52.14"E, elevation 2400-2900m*. Version: 7.3.2.5776 (64-bit).
Google Earth, NASA & Landsat / Copernicus (2002). *Satellite map Fagta Lekoma 8 October 2002, 11° 1'17.73"N, 36°52'52.14"E, elevation 2400-2900m*. Version: 7.3.2.5776 (64-bit).
Haileslassie, A., Priess, J., Veldkamp, E., Teketay, D. & Lesschen, J.P. (2005). Assessment of soil nutrient depletion and its spatial variability on smallholders' mixed farming systems in Ethiopia using partial versus full nutrient balances. *Agriculture, Ecosystems & Environment*, vol. 108 (1), pp. 1–16
Haregeweyn, N., Tsunekawa, A., Nyssen, J., Poesen, J., Tsubo, M., Tsegaye Meshesha, D., Schütt, B., Adgo, E. & Tegegne, F. (2015). Soil erosion and conservation in Ethiopia: A review. *Progress in Physical Geography: Earth and Environment*, vol. 39 (6), pp. 750–774 SAGE Publications Ltd.
Hengl, T., Heuvelink, G.B.M., Kempen, B., Leenaars, J.G.B., Walsh, M.G., Shepherd, K.D., Sila, A., MacMillan, R.A., Jesus, J.M. de, Tamene, L. & Tondoh, J.E. (2015). Mapping Soil Properties of Africa at 250 m Resolution: Random Forests Significantly Improve Current Predictions. *PLOS ONE*, vol. 10 (6), p. e0125814 Public Library of Science.
Hengl, T., Jesus, J.M. de, Heuvelink, G.B.M., Gonzalez, M.R., Kilibarda, M., Blagotić, A., Shangguan, W., Wright, M.N., Geng, X., Bauer-Marschallinger, B., Guevara, M.A., Vargas, R., MacMillan, R.A., Batjes, N.H., Leenaars, J.G.B., Ribeiro, E., Wheeler, I., Mantel, S. & Kempen, B. (2017). SoilGrids250m: Global gridded soil information based on machine learning. *PLOS ONE*, vol. 12 (2), p. e0169748 Public Library of Science.
Her, Y., Frankenberger, J., Chaubey, I. & Srinivasan, R. (2015). Threshold Effects in HRU Definition of the Soil and Water Assessment Tool. *Transactions of the ASABE (American Society of Agricultural and Biological Engineers)*, vol. 58, pp. 367–378
Huffman, R.L., Fangmeier, D.D., Elliot, W.J. & Workman, S.R. (2013). Terraces and Vegetated Waterways. *Soil and Water Conservation Engineering Seventh Edition*. American Society of Agricultural and Biological Engineers, pp. 171–198.
Ilstedt, U., Malmer, A., Verbeeten, E. & Murdiyarso, D. (2007). The effect of afforestation on water infiltration in the tropics: A systematic review and meta-analysis. *Forest Ecology and Management*, vol. 251 (1–2), pp. 45–51
Jarvis, A., Reuter, H.I., Nelson, A. & Guevara, E. (2008). Hole-filled seamless SRTM data V4. Tech. rep., International Centre for Tropical Agriculture (CIAT). Available at: http://srtm.csi.cgiar.org.
Jung, H.C., Getirana, A., Policelli, F., McNally, A., Arsenault, K.R., Kumar, S., Tadesse, T. & Peters-Lidard, C.D. (2017). Upper Blue Nile basin water budget from a multi-model perspective. *Journal of Hydrology*, vol. 555, pp. 535–546
Kebede, S., Travi, Y., Alemayehu, T. & Marc, V. (2006). Water balance of Lake Tana and its sensitivity to fluctuations in rainfall, Blue Nile basin, Ethiopia. *Journal of Hydrology*, vol. 316 (1), pp. 233–247
Kidane, M., Bezie, A., Kesete, N. & Tolessa, T. (2019). The impact of land use and land cover (LULC) dynamics on soil erosion and sediment yield in Ethiopia. *Heliyon*, vol. 5 (12), p. e02981
Kindu, M., Glatzel, G., Tadesse, Y. & Yosef, A. (2006). Tree species screened on nitisols of central Ethiopia: Biomass production, nutrient contents and effect on soil nitrogen. *Journal of Tropical Forest Science*, vol. 18 (3), pp. 173–180 Forest Research Institute Malaysia.
Le Maitre, D.C., Gush, M.B. & Dzikiti, S. (2015). Impacts of invading alien plant species on water flows at stand and catchment scales. *AoB PLANTS*, vol. 7 Oxford Academic. DOI: https://doi.org/10.1093/aobpla/plv043
Leenaars, J.G.B., Claessens, L., Heuvelink, G.B.M., Hengl, T., Ruiperez González, M., van Bussel, L.G.J., Guilpart, N., Yang, H. & Cassman, K.G. (2018). Mapping rootable depth

and root zone plant-available water holding capacity of the soil of sub-Saharan Africa. *Geoderma*, vol. 324, pp. 18–36
Lemann, T., Roth, V. & Zeleke, G. (2017). Impact of precipitation and temperature changes on hydrological responses of small-scale catchments in the Ethiopian Highlands. *Hydrological Sciences Journal*, vol. 62 (2), pp. 270–282 Taylor & Francis.
Lemenih, M. & Kassa, H. (2014). Re-greening Ethiopia: History, challenges and lessons. *Forests*, vol. 5, pp. 1896–1909
Lemma, H., Frankl, A., Griensven, A. van, Poesen, J., Adgo, E. & Nyssen, J. (2019). Identifying erosion hotspots in Lake Tana Basin from a multisite Soil and Water Assessment Tool validation: Opportunity for land managers. *Land Degradation & Development*, vol. 30 (12), pp. 1449–1467
Li, K.Y., Coe, M.T., Ramankutty, N. & Jong, R.D. (2007). Modeling the hydrological impact of land-use change in West Africa. *Journal of Hydrology*, vol. 337 (3), pp. 258–268
Liang, J., Reynolds, T., Wassie, A., Collins, C., Wubalem, A. & 1 Environmental Studies Program, Colby College, Waterville, ME 04901, USA (2016). Effects of exotic Eucalyptus spp. plantations on soil properties in and around sacred natural sites in the northern Ethiopian Highlands. *AIMS Agriculture and Food*, vol. 1 (2), pp. 175–193
Luo, Y., Su, B., Yuan, J., Li, H. & Zhang, Q. (2011). GIS Techniques for Watershed Delineation of SWAT Model in Plain Polders. *Procedia Environmental Sciences*, vol. 10, pp. 2050–2057 (2011 3rd International Conference on Environmental Science and Information Application Technology ESIAT 2011)
Mahfouz, P., Mitri, G., Jazi, M. & Karam, F. (2016). Investigating the Temporal Variability of the Standardized Precipitation Index in Lebanon. *Climate*, vol. 4 (2), p. 27 Multidisciplinary Digital Publishing Institute.
Megerssa, G.R. & Bekere, Y.B. (2019). Causes, consequences and coping strategies of land degradation: evidence from Ethiopia. *Journal of Degraded and Mining Lands Management*, vol. 7 (1), pp. 1953–1957
Mekonnen, K., Yohannes, T., Glatzel, G. & Amha, Y. (2006). Performance of eight tree species in the highland Vertisols of central Ethiopia: growth, foliage nutrient concentration and effect on soil chemical properties. *New Forests*, vol. 32 (3), pp. 285–298
Melaku, N.D., Renschler, C.S., Holzmann, H., Strohmeier, S., Bayu, W., Zucca, C., Ziadat, F. & Klik, A. (2018). Prediction of soil and water conservation structure impacts on runoff and erosion processes using SWAT model in the northern Ethiopian highlands. *Journal of Soils and Sediments*, vol. 18 (4), pp. 1743–1755
Mellander, P.-E., Gebrehiwot, S.G., Gärdenäs, A.I., Bewket, W. & Bishop, K. (2013). Summer Rains and Dry Seasons in the Upper Blue Nile Basin: The Predictability of Half a Century of Past and Future Spatiotemporal Patterns. *PLOS ONE*, vol. 8 (7), p. e68461 Public Library of Science.
Molla, A. & Linger, E. (2017). Effects of Acacia decurrens (Green wattle) Tree on selected Soil Physico-chemical properties North-western Ethiopia. p. 10
Nadal-Romero, E., Cammeraat, E., Pérez-Cardiel, E. & Lasanta, T. (2016). Effects of secondary succession and afforestation practices on soil properties after cropland abandonment in humid Mediterranean mountain areas. *Agriculture, Ecosystems & Environment*, vol. 228, pp. 91–100
NASA (2018). *POWER Data Access Viewer v1.1.1. Prediction of worldwide energy resource*. [Meteorology and solar related data access]. Available at: https://power.larc.nasa.gov/data-access-viewer/?fbclid=IwAR0SUp8HH6cpkHlXEWjEDgKkMbeTuKC6VpfOcbfopW7 kMUCBnrSzpvwYHpU [2020-02-21]
NBI (2016). *Nile Basin Water Resource Atlas* Available at: http://atlas.nilebasin.org/start/
Nigussie, Z., Tsunekawa, A., Haregeweyn, N., Adgo, E., Nohmi, M., Tsubo, M., Aklog, D., Meshesha, D.T. & Abele, S. (2017a). Factors Affecting Small-Scale Farmers' Land Allocation and Tree Density Decisions in an Acacia decurrens-Based taungya System in Fagita Lekoma District, North-Western Ethiopia. *Small-scale Forestry*, vol. 16 (2), pp. 219–233
Nigussie, Z., Tsunekawa, A., Haregeweyn, N., Adgo, E., Nohmi, M., Tsubo, M., Aklog, D., Meshesha, D.T. & Abele, S. (2017b). Factors influencing small-scale farmers' adoption

of sustainable land management technologies in north-western Ethiopia. *Land Use Policy*, vol. 67, pp. 57–64

Nigussie, Z., Tsunekawa, A., Haregeweyn, N., Adgo, E., Tsubo, M., Ayalew, Z. & Abele, S. (2020). Economic and financial sustainability of an Acacia decurrens-based Taungya system for farmers in the Upper Blue Nile Basin, Ethiopia. *Land Use Policy*, vol. 90, p. 104331

Onyutha, C. (2016). Statistical analyses of potential evapotranspiration changes over the period 1930–2012 in the Nile River riparian countries. *Agricultural and Forest Meteorology*, vols. 226–227, pp. 80–95

Péllico Netto, S., Sanquetta, C.R., Caron, B.O., Behling, A., Simon, A.A., Corte, A.P.D. & Bamberg, R. (2015). Ground level photosynthetically active radiation dynamics in stands of Acacia mearnsii De Wild. *Anais da Academia Brasileira de Ciências*, vol. 87 (3), pp. 1833–1845

Rockström, J., Barron, J. & Fox, P. (2003). Water productivity in rain-fed agriculture: challenges and opportunities for smallholder farmers in drought-prone tropical agroecosystems. In: Kijne, J.W., Barker, R., & Molden, D. (eds.) *Water productivity in agriculture: limits and opportunities for improvement*. Wallingford: CABI, pp. 145–162.

Senkondo, W. (2018). On the evolution of hydrological modelling for water resources in Eastern Africa. *CAB Reviews: Perspectives in Agriculture, Veterinary Science, Nutrition and Natural Resources*, vol. 13 (028). DOI: https://doi.org/10.1079/PAVSNNR201813028

Senkondo, W. (2020). *Modelling water resources despite data limitations in Tanzania's Kilombero Valley*. (Academic dissertation for the Degree of Doctor of Philosophy). Stockholm University.

Senkondo, W., Munishi, S.E., Tumbo, M., Nobert, J. & Lyon, S.W. (2019). Comparing Remotely-Sensed Surface Energy Balance Evapotranspiration Estimates in Heterogeneous and Data-Limited Regions: A Case Study of Tanzania's Kilombero Valley. *Remote Sensing*, vol. 11 (11), p. 1289 Multidisciplinary Digital Publishing Institute.

Senkondo, W., Tumbo, M. & Lyon, S.W. (2018). On the evolution of hydrological modelling for water resources in Eastern Africa. *CAB Reviews*, vol. 13 (028), pp. 1–26 CABI.

Setegn, S.G., Srinivasan, R. & Dargahi, B. (2008). Hydrological Modelling in the Lake Tana Basin, Ethiopia Using SWAT Model. *The Open Hydrology Journal*, vol. 2 (1), pp. 49–62

Shiferaw, B. & Holden, S. (1999). Soil Erosion and Smallholders' Conservation Decisions in the Highlands of Ethiopia. *World Development*, vol. 27 (4), pp. 739–752

Sisay, K., Thurnher, C. & Hasenauer, H. (2017). Daily climate data for the Amhara region in Northwestern Ethiopia. *International Journal of Climatology*, vol. 37 (6), pp. 2797–2808

S.L. Neitsch, J.G. Arnold, J.R. Kiniry & J.R. Williams (2011). *Soil and water assessment tool - theoretical documentation Version 2009*. (Texas Water Resources Institute Technical Report No. 406). Texas, USA: Texas A and M University.

Tadesse, A. (2020). *Assessment of water infiltration rate under different land use practic at Fagita Lekoma District of Amhara Regional State, Ethiopia*. (Master thesis). University of Gondar.

Tadesse, W., Gezahgne, A., Tesema, T., Shibabaw, B., Tefera, B. & Kassa, H. (2019). Plantation Forests in Amhara Region: Challenges and Best Measures for Future Improvements. *World Journal of Agricultural Research*, vol. 7 (4), p. 9

Tebebu, T.Y., Steenhuis, T.S., Dagnew, D.C., Guzman, C.D., Bayabil, H.K., Zegeye, A.D., Collick, A.S., Langan, S., MacAlister, C., Langendoen, E.J., Yitaferu, B. & Tilahun, S.A. (2015). Improving efficacy of landscape interventions in the (sub) humid Ethiopian highlands by improved understanding of runoff processes. *Frontiers in Earth Science*, vol. 3 Frontiers. DOI: https://doi.org/10.3389/feart.2015.00049

Tekleab, S., Uhlenbrook, S., Mohamed, Y., Savenije, H.H.G., Temesgen, M. & Wenninger, J. (2011). Water balance modeling of Upper Blue Nile catchments using a top-down approach. *Hydrology and Earth System Sciences*, vol. 15 (7), pp. 2179–2193

Tesemma, Z.K., Mohamed, Y.A. & Steenhuis, T.S. (2010). Trends in rainfall and runoff in the Blue Nile Basin: 1964–2003. *Hydrological Processes*, vol. 24 (25), pp. 3747–3758

Tesfaye, G., Debebe, Y. & Fikirie, K. (2018). Soil Erosion Risk Assessment Using GIS Based USLE Model for Soil and Water Conservation Planning in Somodo Watershed, South West Ethiopia. *International Journal of Environmental & Agriculture Research*, vol. 4 (5), pp. 35–43

Tesfaye, M.A., Bravo-Oviedo, A., Bravo, F., Kidane, B., Bekele, K. & Sertse, D. (2015). Selection of Tree Species and Soil Management for Simultaneous Fuelwood Production and Soil Rehabilitation in the Ethiopian Central Highlands. *Land Degradation & Development*, vol. 26 (7), pp. 665–679

Tsegay, A., Raes, D., Geerts, S., Vanuytrecht, E., Abraha, B., Deckers, J., Bauer, H. & Gebrehiwot, K. (2012). Unravelling crop water productivity of teff (Eragrostis tef (Zucc.) Trotter) through AquaCrop in Northern Ethiopia. *Experimental Agriculture*, vol. 48 (2), pp. 222–237

Tully, K., Sullivan, C., Weil, R. & Sanchez, P. (2015). The State of Soil Degradation in Sub-Saharan Africa: Baselines, Trajectories, and Solutions. *Sustainability*, vol. 7 (6), pp. 6523–6552 Multidisciplinary Digital Publishing Institute.

USDA Agricultural Research Service*Soil - Plant - Air -Water tool Field and Pond Hydrology V.6.02.75*.

USDA-Agricultural Research Service (2013). *Revised Universal Soil Loss Equation version 2 (RUSLE2)*. Washington, D.C.: USDA - Agricultural Research Service.

Vigiak, O., Malagó, A., Bouraoui, F., Vanmaercke, M. & Poesen, J. (2015). Adapting SWAT hillslope erosion model to predict sediment concentrations and yields in large Basins. *Science of The Total Environment*, vol. 538, pp. 855–875

Waidler, D., White, M., Steglich, E., Wang, S., Williams, J., Jones, C.A. & Srinivasan, R. (2009). *Conservation-Practice-Modeling-Guide for SWAT and APEX* Available at: https://swat.tamu.edu/media/57882/Conservation-Practice-Modeling-Guide.pdf [2020-04-23]

Winchell, M., Srinivasan, R., Di Luzio, M. & Arnold, J. (2013). *ArcSWAT interface for SWAT 2012*. Temple, Texas: Texas Agrilife Research and USDA agricultural research service.

Wondie, M. & Mekuria, W. (2018). Planting of Acacia decurrens and Dynamics of Land Cover Change in Fagita Lekoma District in the Northwestern Highlands of Ethiopia. *Mountain Research and Development*, vol. 38 (3), pp. 230–239 International Mountain Society.

Worqlul, A.W., Ayana, E.K., Yen, H., Jeong, J., MacAlister, C., Taylor, R., Gerik, T.J. & Steenhuis, T.S. (2018). Evaluating hydrologic responses to soil characteristics using SWAT model in a paired-watersheds in the Upper Blue Nile Basin. *CATENA*, vol. 163, pp. 332–341

Zegeye, A.D., Langendoen, E.J., Tilahun, S.A., Mekuria, W., Poesen, J. & Steenhuis, T.S. (2018). Root reinforcement to soils provided by common Ethiopian highland plants for gully erosion control. *Ecohydrology*, vol. 11 (6), p. e1940

Zeleke, G. & Hurni, H. (2001). Implications of Land Use and Land Cover Dynamics for Mountain Resource Degradation in the Northwestern Ethiopian Highlands. *Mountain Research and Development*, vol. 21 (2), pp. 184–191 International Mountain Society.

Appendix A. Input tables soil physical properties

The tables 15 - 20 is this appendix are the soil physical parameters used in the SWAT model based on the different soil maps (Hengl *et al.* 2015; Leenaars *et al.* 2018), where BD is the bulk density, AWC is the available water capacity, K is the saturated hydraulic conductivity, CBN is the carbon content, ALB is the soil albedo and USLE_K is the erodibility factor.

Table 15. Soil physical properties used in the SWAT model for the first soil layer (Hengl et al. *2015; Leenaars* et al. *2018).*

SUB-BASIN	SOL_BD1	SOL_AWC1	SOL_K1	SOL_CBN1	CLAY1	SILT1	SAND1	ROCK1	SOL_ALB1	USLE_K1
1	1.094	0.13	2.5	3.02	44	31	25	9	0.17	0.14
2	1.088	0.13	2.2	3.15	46	30	24	11	0.17	0.12
3	1.089	0.13	2.9	3.41	44	32	24	7	0.17	0.13
4	1.064	0.13	2.5	3.31	44	30	26	9	0.17	0.12
5	1.074	0.13	2.4	3.18	45	31	25	13	0.17	0.13
6	1.049	0.13	3.0	3.47	43	31	26	6	0.17	0.13
7	1.072	0.13	2.5	3.83	47	30	23	9	0.17	0.11
8	1.075	0.13	2.3	3.08	46	31	23	8	0.17	0.13
9	1.062	0.13	2.7	3.68	45	30	25	7	0.17	0.11
10	1.050	0.13	2.2	3.19	45	29	26	5	0.17	0.12
11	1.080	0.13	2.4	3.41	46	30	24	6	0.17	0.12
12	1.073	0.13	2.1	3.03	46	29	24	10	0.17	0.12
13	1.085	0.13	2.1	3.15	47	30	23	8	0.17	0.12
14	1.085	0.13	1.9	3.05	49	30	21	7	0.17	0.11
15	1.061	0.13	2.7	3.65	45	30	25	6	0.17	0.12
16	1.049	0.13	2.4	3.45	46	30	24	6	0.17	0.12
17	1.072	0.13	2.5	3.43	45	30	25	8	0.17	0.12
18	1.053	0.13	2.5	3.62	46	30	24	5	0.17	0.11
19	1.066	0.13	2.7	3.61	44	30	26	7	0.17	0.12
20	1.051	0.13	2.9	3.86	45	30	24	5	0.17	0.11
21	1.079	0.13	2.8	3.73	44	30	26	9	0.17	0.12
22	1.040	0.13	2.9	4.20	46	29	24	6	0.17	0.09
23	1.098	0.13	2.0	3.13	47	30	24	8	0.17	0.12
24	1.063	0.13	2.2	3.64	47	30	24	7	0.17	0.11
25	1.076	0.13	2.1	3.09	45	29	27	7	0.17	0.13

SUB-BASIN	SOL_BD1	SOL_AWC1	SOL_K1	SOL_CBN1	CLAY1	SILT1	SAND1	ROCK1	SOL_ALB1	USLE_K1
26	1.111	0.13	2.9	3.59	43	30	27	9	0.17	0.12
27	1.092	0.13	2.7	3.52	43	30	28	9	0.17	0.12

Table 16. Soil physical properties used in the SWAT model for the second soil layer (Hengl et al. 2015; Leenaars et al. 2018).

SUB-BASIN	SOL_Z2	SOL_BD2	SOL_AWC2	SOL_K2	SOL_CBN2	CLAY2	SILT2	SAND2	ROCK2
1	150	1.103	0.13	2.0	2.66	46	30	24	8
2	150	1.100	0.13	1.8	2.70	48	30	22	10
3	150	1.094	0.13	2.2	2.85	46	31	23	6
4	150	1.071	0.13	2.1	2.85	45	30	25	8
5	150	1.079	0.13	2.1	2.76	46	30	23	12
6	150	1.049	0.13	2.5	2.99	44	30	25	5
7	150	1.072	0.13	2.1	3.18	48	30	22	8
8	150	1.077	0.13	1.8	2.64	47	30	23	7
9	150	1.061	0.13	1.9	3.01	47	30	24	6
10	150	1.050	0.13	1.8	2.73	47	29	24	4
11	150	1.079	0.13	1.8	2.80	48	29	23	6
12	150	1.070	0.13	1.7	2.63	48	29	23	9
13	150	1.085	0.13	1.6	2.66	49	29	22	7
14	150	1.084	0.13	1.7	2.59	50	29	20	6
15	150	1.063	0.13	1.9	3.01	47	29	24	5
16	150	1.053	0.13	1.8	2.96	48	29	23	5
17	150	1.074	0.13	1.9	2.89	47	30	24	7
18	150	1.056	0.13	1.8	3.03	48	30	23	5
19	150	1.068	0.13	2.1	2.98	46	29	24	6
20	150	1.055	0.13	2.1	3.20	47	30	23	4
21	150	1.080	0.13	2.1	3.13	46	29	25	8
22	150	1.040	0.13	2.1	3.50	48	29	23	5
23	150	1.099	0.13	1.7	2.71	48	29	23	7
24	150	1.064	0.13	1.9	3.06	48	29	23	6
25	150	1.076	0.13	1.7	2.66	47	28	25	7
26	150	1.112	0.13	2.4	3.01	44	30	26	8
27	150	1.093	0.13	2.3	2.89	44	29	26	8

Table 17. Soil physical properties used in the SWAT model for the third soil layer (Hengl et al. 2015; Leenaars et al. 2018).

SUB-BASIN	SOL_Z3	SOL_BD3	SOL_AWC3	SOL_K3	SOL_CBN3	CLAY3	SILT3	SAND3	ROCK3
1	300	1.147	0.13	1.5	2.34	48	28	23	11
2	300	1.148	0.13	1.3	2.43	51	28	22	12
3	300	1.145	0.13	1.6	2.51	49	29	22	8
4	300	1.114	0.13	1.5	2.52	48	28	24	10
5	300	1.112	0.12	1.4	2.43	50	28	22	14
6	300	1.072	0.13	1.5	2.59	49	28	23	6
7	300	1.084	0.12	1.5	2.71	51	28	21	10
8	300	1.102	0.12	1.3	2.33	51	28	21	9
9	300	1.076	0.12	1.5	2.66	50	28	22	8
10	300	1.055	0.12	1.3	2.43	50	27	23	6
11	300	1.089	0.12	1.3	2.37	51	27	21	8
12	300	1.076	0.12	1.2	2.23	51	27	22	11
13	300	1.095	0.12	1.2	2.27	52	27	21	8
14	300	1.095	0.12	1.2	2.27	52	27	21	8
15	300	1.072	0.12	1.4	2.54	50	28	22	7
16	300	1.060	0.12	1.4	2.52	51	28	21	7
17	300	1.091	0.12	1.4	2.48	50	28	22	9
18	300	1.063	0.12	1.4	2.64	51	28	21	6
19	300	1.075	0.12	1.5	2.62	49	28	23	8
20	300	1.064	0.12	1.7	2.75	49	29	22	6
21	300	1.088	0.13	1.6	2.59	48	28	24	12
22	300	1.060	0.12	1.6	2.80	50	29	21	7
23	300	1.107	0.12	1.2	2.29	51	28	22	10
24	300	1.073	0.12	1.5	2.59	50	28	22	9
25	300	1.081	0.13	1.3	2.32	49	27	24	9
26	300	1.120	0.13	1.7	2.39	46	29	25	12
27	300	1.102	0.13	1.6	2.44	47	28	25	11

Table 18. Soil physical properties used in the SWAT model for the fourth soil layer (Hengl et al. 2015; Leenaars et al. 2018).

SUB-BASIN	SOL_Z4	SOL_BD4	SOL_AWC4	SOL_K4	SOL_CBN4	CLAY4	SILT4	SAND4	ROCK4
1	600	1.176	0.12	0.8	1.48	54	25	21	14
2	600	1.173	0.12	0.7	1.50	57	24	20	13
3	600	1.176	0.11	0.7	1.67	58	23	19	10
4	600	1.149	0.12	0.7	1.53	56	23	21	12
5	600	1.153	0.12	0.8	1.59	56	24	20	16
6	600	1.127	0.12	0.7	1.58	57	24	20	9
7	600	1.124	0.11	0.7	1.77	59	23	18	11
8	600	1.151	0.12	0.7	1.52	58	24	19	11
9	600	1.128	0.11	0.7	1.72	58	23	19	9
10	600	1.090	0.12	0.6	1.52	57	23	21	9
11	600	1.129	0.11	0.6	1.63	59	22	19	9
12	600	1.118	0.12	0.6	1.51	58	22	20	13
13	600	1.114	0.11	0.7	1.53	59	23	18	10
14	600	1.114	0.11	0.7	1.53	59	23	18	10
15	600	1.093	0.11	0.7	1.72	58	23	19	9
16	600	1.083	0.11	0.7	1.68	58	24	19	10
17	600	1.122	0.12	0.7	1.64	57	24	20	11
18	600	1.084	0.11	0.7	1.73	58	24	19	9
19	600	1.095	0.12	0.7	1.71	56	23	21	11
20	600	1.091	0.12	0.9	1.78	56	25	19	7
21	600	1.111	0.12	0.8	1.76	55	24	21	14
22	600	1.080	0.12	0.9	1.80	57	25	18	7
23	600	1.128	0.12	0.7	1.58	57	23	20	13
24	600	1.101	0.12	0.9	1.83	56	25	19	11
25	600	1.101	0.12	0.6	1.59	56	23	22	11
26	600	1.156	0.13	1.1	1.70	50	27	23	16
27	600	1.122	0.12	0.8	1.67	54	23	22	14

Table 19. Soil physical properties used in the SWAT model for the fifth soil layer (Hengl et al. 2015; Leenaars et al. 2018).

SUB-BASIN	SOL_Z5	SOL_BD5	SOL_AWC5	SOL_K5	SOL_CBN5	CLAY5	SILT5	SAND5	ROCK5
1	1000	1.268	0.12	0.7	0.97	55	23	21	15
2	1000	1.270	0.12	0.6	0.98	59	22	19	15
3	1000	1.239	0.12	0.5	1.01	60	21	19	11
4	1000	1.235	0.12	0.5	0.97	57	22	21	13
5	1000	1.213	0.12	0.5	1.03	59	22	20	18
6	1000	1.189	0.12	0.6	1.00	58	22	20	10
7	1000	1.174	0.12	0.7	1.22	61	21	18	12
8	1000	1.208	0.12	0.5	1.03	60	22	19	13
9	1000	1.184	0.11	0.6	1.19	61	21	18	10
10	1000	1.153	0.12	0.5	1.11	59	21	20	10
11	1000	1.182	0.11	0.6	1.15	62	20	18	11
12	1000	1.172	0.12	0.5	1.08	60	20	20	15
13	1000	1.167	0.11	0.6	1.15	61	21	18	13
14	1000	1.167	0.11	0.6	1.15	61	21	18	13
15	1000	1.153	0.11	0.5	1.29	61	21	19	10
16	1000	1.134	0.11	0.6	1.18	60	22	18	11
17	1000	1.184	0.12	0.6	1.15	59	22	19	12
18	1000	1.142	0.11	0.6	1.23	60	22	18	10
19	1000	1.165	0.12	0.6	1.29	58	22	20	13
20	1000	1.152	0.12	0.7	1.26	58	24	18	9
21	1000	1.175	0.12	0.6	1.29	57	23	21	15
22	1000	1.120	0.12	0.7	1.30	59	24	17	7
23	1000	1.191	0.12	0.6	1.18	59	22	19	13
24	1000	1.169	0.12	0.7	1.32	58	23	19	12
25	1000	1.162	0.12	0.6	1.19	57	21	21	13
26	1000	1.209	0.12	0.8	1.25	52	25	23	16
27	1000	1.183	0.12	0.6	1.23	56	22	22	15

Table 20. Soil physical properties used in the SWAT model for the sixth soil layer (Hengl et al. 2015; Leenaars et al. 2018).

SUB-BASIN	SOL_Z6	SOL_BD6	SOL_AWC6	SOL_K6	SOL_CBN6	CLAY6	SILT6	SAND6	ROCK6
1	2000	1.297	0.12	0.6	6.74	55	23	22	18
2	2000	1.300	0.12	0.6	0.69	57	22	21	18
3	2000	1.264	0.12	0.5	0.69	59	21	20	13
4	2000	1.283	0.12	0.5	0.66	56	21	23	16
5	2000	1.265	0.12	0.5	0.73	57	21	22	19
6	2000	1.252	0.12	0.5	0.63	57	21	22	13
7	2000	1.219	0.12	0.6	0.75	61	20	19	14
8	2000	1.278	0.12	0.5	0.65	59	21	20	14
9	2000	1.231	0.12	0.5	0.68	60	20	19	12
10	2000	1.212	0.41	0.4	0.68	58	20	22	14
11	2000	1.223	0.12	0.5	0.66	61	19	20	13
12	2000	1.234	0.38	0.4	0.68	60	19	21	17
13	2000	1.205	0.12	0.5	0.70	61	20	19	14
14	2000	1.205	0.12	0.5	0.70	61	20	19	14
15	2000	1.187	0.12	0.4	0.71	61	20	20	12
16	2000	1.182	0.12	0.4	0.64	60	21	20	13
17	2000	1.226	0.12	0.4	0.69	58	21	21	15
18	2000	1.182	0.12	0.5	0.65	60	21	19	12
19	2000	1.207	0.12	0.4	0.76	58	21	22	15
20	2000	1.193	0.12	0.5	0.68	58	22	20	10
21	2000	1.204	0.12	0.5	0.75	56	22	22	17
22	2000	1.170	0.12	0.6	0.70	58	23	19	9
23	2000	1.225	0.12	0.5	0.69	59	21	20	16
24	2000	1.204	0.12	0.5	0.70	58	23	20	14
25	2000	1.201	0.12	0.4	0.72	57	20	23	15
26	2000	1.242	0.13	0.6	0.74	52	24	24	20
27	2000	1.209	0.12	0.5	7.60	56	21	23	18

Appendix B. Crop parameters *Acacia decurrens* and teff

The tables 21 – 24 in this appendix are the crop parameters defined for the *A. decurrens* and the database values for teff. For teff only the root depth has been altered.

Table 21. Crop parameters defined for the Acacia decurrens.

Description	Parameter	Value	Unit	Source
Growth period of the tree crops		5.33	Year	(Clulow et al. 2011; Le Maitre et al. 2015)
Land cover/plant classification	IDC	6. Perennial	(-)	
Radiation-use efficiency	BIO_E	25	(kg/ha)/(MJ/m^2)	(Péllico Netto et al. 2015)
Harvest index for optimal growing conditions	HVSTI	0.76	(kg/ha)/(kg/ha)	(Arnold *et al.* 2012a)
Lower limit of harvest index	WSYF	0.01	(kg/ha)/(kg/ha)	(Arnold *et al.* 2012a)
Maximum potential leaf area index (LAI) and two fractions of the max. LAI on the optimal leaf area development curve.	BLAI FRGRW1 LAIMX1 FRGRW2 LAIMX2	3.5 0.1 0.05 0.4 0.95	(-) (-) (-) (-) (-)	(Dye & Jarmain 2004; Bulcock & Jewitt 2010; Arnold *et al.* 2012a; Le Maitre *et al.* 2015)
Fraction of growing season when leaf area begins to decline	DLAI	0.99	(-)	(Arnold *et al.* 2012a)
Max. canopy height	CHTMX	12	Meter	(Kindu et al. 2006; Mekonnen et al. 2006; Tesfaye et al. 2015; Endalamaw 2019; Ferede et al. 2019; Amha et al. 2020)
Max. root depth	RDMX	1.0	Meter	(Belayneh *et al.* 2018; Zegeye *et al.* 2018)
Optimal temperature for plant growth	T_OPT	20	°C	(Ethiopian National Meteorology Agency; Gelaro *et al.* 2017)
Minimum temperature for plant growth	T_BASE	8	°C	(Arnold *et al.* 2012a)
Normal fraction of N in yield	CNYLD	0.003	Kg N/kg yield	(Kindu et al. 2006)
Normal fraction of P in yield	CPYLD	0.0001	Kg P/kg yield	(Kindu et al. 2006)

Table 22. Crop parameters defined for the Acacia decurrens 2.

Description	Parameter	Value	Unit	Source
N and P uptake parameters at emergence, at 50% maturity and at maturity.	PLTNFR1 PLTPFR1 PLTNFR2 PLTPFR2 PLTNFR3 PLTPFR3	0.0012 0.00023 0.0004 0.00013 0.0003 0.0001	Kg N/kg biomass & Kg P/kg biomass	(Kindu *et al.* 2006; Arnold *et al.* 2012a)
Minimum value of USLE C factor for water erosion applicable to the land cover/plant	USLE_C	0.001	(-)	(Bewket & Teferi 2009; Arnold *et al.* 2012a; Tesfaye *et al.* 2018)
Maximum stomatal conductance	GSI	0.0036	m/s	(Arnold *et al.* 2012a)
Rate of decline in RUE per unit increase in vapor pressure deficit	WAVP	8	(kg/ha)/(MJ/m^2)	(Arnold *et al.* 2012a)
Elevated CO_2 atmospheric conc. corresponding to the 2nd point on the RUE curve	CO2HI	660	µL CO_2/L air	(Arnold *et al.* 2012a)
Biomass-energy ratio corresponding to the 2nd point on the RUE curve	BIOEHI	26	(-)	(Péllico Netto et al. 2015)
Plant residue decomposition coefficient	RSDCO_PL	0.05	(-)	(Arnold *et al.* 2012a)
Max. biomass for forest	BMX_TREES	15	Metric t/ha	(Kindu et al. 2006; Asmare & Gure 2019; Ferede et al. 2019)
Biomass die-off fraction	BMDIEOFF	0.10	(-)	(Arnold *et al.* 2012a)
Root to shoot ratio at the beginning of the growing season	RSR1C	0.40	(-)	(Arnold *et al.* 2012a)
Root to shoot ratio at the end of the growing season	RSR2C	0.20	(-)	(Arnold *et al.* 2012a)
Light extinction coefficient	EXT_COEF	0.65	(-)	(Clulow *et al.* 2011; Arnold *et al.* 2012a)

Table 23. Crop parameters for teff based on the crop database in SWAT (Arnold et al. *2012a).*

Description	Parameter	Value	Unit	Source
Growth period of the tree crops		5	Months	(Arnold *et al.* 2012a)
Land cover/plant classification	IDC	5. Cold seasonal annual	(-)	(Arnold *et al.* 2012a)
Radiation-use efficiency	BIO_E	35	(kg/ha)/(MJ/m^2)	(Arnold *et al.* 2012a)
Harvest index for optimal growing conditions	HVSTI	0.23	(kg/ha)/(kg/ha)	(Arnold *et al.* 2012a)
Lower limit of harvest index	WSYF	0.2	(kg/ha)/(kg/ha)	(Arnold *et al.* 2012a)
Maximum potential leaf area index (LAI) and two fractions of the max. LAI on the optimal leaf area development curve.	BLAI FRGRW1 LAIMX1 FRGRW2 LAIMX2	3.0 0.15 0.05 0.50 0.95	(-) (-) (-) (-) (-)	(Arnold *et al.* 2012a)

Table 24. Crop parameters for teff based on the crop database in SWAT (Arnold et al. 2012a) 2.

Description	Parameter	Value	Unit	Source
Fraction of the growing season when leaf area begins to decline	DLAI	0.90	(-)	(Arnold *et al.* 2012a)
Max. canopy height	CHTMX	0.9	Meter	(Arnold *et al.* 2012a)
Max. root depth	RDMX	0.75	Meter	(Ayele *et al.* 2001; Tsegay *et al.* 2012)
Optimal temperature for plant growth	T_OPT	18	°C	(Arnold *et al.* 2012a)
Minimum temperature for plant growth	T_BASE	0	°C	(Arnold *et al.* 2012a)
Normal fraction of N in yield	CNYLD	0.0234	Kg N/kg yield	(Arnold *et al.* 2012a)
Normal fraction of P in yield	CPYLD	0.0033	Kg P/kg yield	(Arnold *et al.* 2012a)
N and P uptake parameters at emergence, at 50% maturity and at maturity.	PLTNFR1 PLTPFR1 PLTNFR2 PLTPFR2 PLTNFR3 PLTPFR3	0.06 0.0084 0.0231 0.0032 0.0134 0.0019	Kg N/kg biomass & Kg P/kg biomass	(Arnold *et al.* 2012a)
Minimum value of USLE C factor for water erosion applicable to the land cover/plant	USLE_C	0.03	(-)	(Arnold *et al.* 2012a)
Maximum stomatal conductance	GSI	0.0056	m/s	(Arnold *et al.* 2012a)
Rate of decline in RUE per unit increase in vapor pressure deficit	WAVP	8	(kg/ha)/(MJ/m^2)	(Arnold *et al.* 2012a)
Elevated CO_2 atmospheric conc. corresponding to the 2nd point on the RUE curve	CO2HI	660	µL CO_2/L air	(Arnold *et al.* 2012a)
Biomass-energy ratio corresponding to the 2nd point on the RUE curve	BIOEHI	46	(-)	(Arnold *et al.* 2012a)
Plant residue decomposition coefficient	RSDCO_PL	0.05	(-)	(Arnold *et al.* 2012a)
Max. biomass for forest	BMX_TREES	0	Metric t/ha	(Arnold *et al.* 2012a)
Biomass die-off fraction	BMDIEOFF	0.10	(-)	(Arnold *et al.* 2012a)
Root to shoot ratio at the beginning of the growing season	RSR1C	0.	(-)	(Arnold *et al.* 2012a)
Root to shoot ratio at the end of the growing season	RSR2C	0.	(-)	(Arnold *et al.* 2012a)
Light extinction coefficient	EXT_COEF	0.65	(-)	(Arnold *et al.* 2012a)

Appendix C. Soil loss per land use and slope class

Table 25 shows the soil loss values and the sediments yields calculated in SWAT for the different land uses and slope classes, where, ADEC is the *A. decurrens*, FRST is the forest land use, PAST is pasture and TEFF is the cropland planted with teff.

Table 25. Mean annual soil loss in t ha^{-1} y^{-1} for the different land uses and slopes for the control, control with improved SWC practice and afforestation scenario. ADEC; A. decurrens, FRST; forest, PAST; pasture, TEFF; teff.

Land use	Slope (%)	Mean annual soil loss (t ha^{-1} yr^{-1})			Mean annual sediment yield (t ha^{-1} yr^{-1})		
		2002		2019	2002		2019
		Control	SWC	Afforestation	Control	SWC	Afforestation
ADEC	0-5	-		1.8	-		0.9
ADEC	5-12	-		2.5	-		1.5
ADEC	12-20	-		3.5	-		2.5
ADEC	20-30	-		4.1	-		2.8
ADEC	>30	-		5.3	-		3.0
FRST	0-5	0.02		0.03	0.01		0.02
FRST	5-12	0.09		0.10	0.07		0.07
FRST	12-20	0.1		0.1	0.1		0.1
FRST	20-30	0.2		0.2	0.2		0.2
FRST	>30	-		0.3	-		0.2
PAST	0-5	0.08		0.10	0.05		0.06
PAST	5-12	0.3		0.4	0.2		0.2
PAST	12-20	0.4		0.5	0.3		0.3
PAST	20-30	0.6		0.7	0.5		0.5
TEFF	0-5	3.2	1.3	9.4	1.3	0.9	7.1
TEFF	5-12	33.2	12.7	27.9	29.5	10.4	23.6
TEFF	12-20	40.8	20.9	37.8	38.6	17.9	33.5
TEFF	20-30	83.8	78.5	71.1	75.5	63.6	59.4

Appendix D. *Acacia decurrens* height and biomass

Height, diameter at breast height and total dry biomass of the *A. decurrens* as reported in several different studies (table 26). Studies have been conducted on plantations of different ages.

Table 26. Average height, DBH and dry-biomass for the A. decurrens.

Age of plantations (year)	Height (m)	Average DBH (cm)	Total dry-biomass kg/tree	Sources
1	2.8		1.1	(Mekonnen *et al.* 2006)
2	5.1			
3	6.9			
3.5			31.0	
5.5	9.7		35.8	
0.5	0.4			(Amha *et al.* 2020)
1	1.2			
1.5	1.6			
2.5	2.3			
1	1.5		0.02	(Kindu *et al.* 2006)
2	5.3			
3	9.0			
5.5	11.3		11.9	
1	1.0			(Tesfaye *et al.* 2015)
4	6.5			
1.5	2.6	1.2		(Ferede *et al.* 2019)
2.5	6.0	3.0		
3.5	8.5	4.8		
4.5	10.6	5.9		
5.5	11.7	6.3		
5		9.9		(Endalamaw 2019)